rTMS, which was efficacious in treating writer's cramp (9).

2. Materials and methods

2. 1. Subjects

Twelve healthy right- handed male volunteers (33.0± 9.5 years) participated in this study. All subjects were free from neurological and phychiatric diseases. They gave their informed consent for the study, which was approved by the Ethics Committee of the University of Tokushima. Handedness was established by a detailed questionnaire, the Edinburgh Handedness Inventory (10).

2. 2. Experimental design

In an electrically and auditory shielded room, the subjects relaxed on a reclining chair with their feet on the foot-rest and were instructed to keep eyes open. SEPs were recorded before and after application of monophasic 0.2 Hz rTMS or sham stimulation over the left cortex hand motor area. Two sessions (rTMS; real *vs.* sham) were performed on each separate day in a counterbalanced order at 1 week or longer intervals for each session.

2. 3. rTMS

In monophasic rTMS, we used the figure-of-eight stimulation coil (outside diameter of one half-coil, 8.7 cm; Magstim Col Ltd., OHR Wales, UK) connected to Magstim 200 stimulator (2.2 T at the coil surface). Magnetic stimuli of 250 times were delivered at 0.2 Hz to the right motor cortex, 2 cm anterior and 3.5 cm lateral to Cz (International 10- 20 System). We determined the optimal position for activation of the left first dorsal interosseous muscle by moving the coil in 0.5 cm steps around the presumed motor area. Motor response was recorded using electromyography. Threshold was defined as minimum stimulation level necessary to evoke motor response of > 50 μV peak-to-peak amplitude in five out of ten trials. The coil was positioned tangentially to the curvature of the head and handle of the coil formed a 45° angle with subject's body midline. Stimulation intensity was 85 % of the resting motor threshold for the motor cortex.

Sham stimulation was performed by the same procedure as that of rTMS using a figure-of-eight sham coil (a placebo system; Magstim Co. Ltd., OHR Wales, UK; the same shape as that of a true coil) connected to Magstim 200 Stimulator (0.44 tesla at coil surface).

These parameters of rTMS were in accordance with the international safety guidelines (11).

2. 4. SEPs

SEPs were obtained by electric median nerve stimulation at right or left wrist respectively in each session. Each recording took for about 10 minutes. Sides of stimulation were randomly assigned. Electric stimuli (0.2 ms duration) were delivered at 1 Hz through surface electrodes. Positive electrodes were placed on distal and negative ones were on proximal side of wrist. Intensity was adjusted just above the motor threshold of abductor polices muscle. SEPs were recorded with silver chloride disk surface electrodes at F3, F4, 2 cm posterior to C3 (C3') and 2 cm posterior to C4 (C4'), according to the International 10- 20 system. The linked earlobe electrodes served as reference. The impedance of these electrodes were kept below 5 kΩ. The electrooculogram (EOG) was also recorded with a pair of silver chloride disk electrodes at 2 cm above the left outer canthus and 2 cm below the right outer canthus. Signals from scalp electrodes and EOG were amplified and acquired at a sampling rate of 10 kHz and filtered at 1- 5000 Hz and 0.5- 1000 Hz respectively (MEB2200 amplifier; Nihon Kohden, Tokyo, Japan). All signals were recorded for 100 ms after the onset of median nerve stimulation and stored on a personal computer for off-line analysis. We collected at least 200 artifact-free sweeps and then averaged them on off-line.

2. 5. Data analysis

Components with clear peak were all analyzed. Among SEP components from right median nerve stimulation, P14, P22, N30 and N60 were determined at F3; P14, N20, P26, N34 and P45 at C3'; P14, P22 and N30 at F4; P14 was at C4'. Among left median SEP components, P14, P22, N30 and N60 were determined at F4; P14, N20, P26, N34, and P45 at C4'; P14, P22 and N30 at F3; P14 was at C3'. We measured the baseline-to-peak amplitudes of these components. The baseline was defined as the segment between 2 and 6 ms after electrical stimulation.

We analyzed the amplitudes of all SEP components by two- way repeated measures analysis of variance (ANOVA) with conditions (real *vs.* sham rTMS stimulation) and time

course (before *vs.* after stimulation). When statistical significance was reached, we used two tail paired t-test to analyze the amplitude change after rTMS compared with that of before.

All data were analyzed with SPSS version 11.01 J for Windows (SPSS Japan Institute Inc., Tokyo). Significant level of all analysis were defined $p < 0.05$.

3. Results

Figure 1 shows the grand-averaged waveforms obtained from twelve subjects. Table 1 shows the peak amplitudes of each component before and after application of rTMS and sham stimulation. In rTMS condition, only N34 amplitude at C3' of right median SEPs reached a significance level by repeated measures ANOVA ($F = 4.585$, $p = 0.044$). Post hoc analysis disclosed N34 amplitude after rTMS increased significantly ($t = -3.332$, $p = 0.007$) (Fig 2). Figure 3 shows the amplitude change of the N34 component of SEPs by right and left median nerve stimulation before and after rTMS in each subject. Right median nerve stimulation disclosed significant change of N34 amplitude though left median nerve stimulation showed no significant change. Any components of left median SEPs did not change, or sham stimulation showed no changes of SEPs in each stimulation side.

4. Discussion

Our results showed that monophasic very low-frequency (0.2 Hz) rTMS over the right motor cortex increased the amplitude of N34 component recorded from the left scalp (C3') after right median nerve stimulation. In previous studies, rTMS over the primary motor cortex modified the excitability of the contralateral primary motor cortex (12, 13). This study for the first time showed the rTMS predominantly affects the contralateral SEP component, while leaving the ipsilateral ones unaffected.

Bilateral motor cortices are basically considered to transfer inhibitory effect upon each other (transcallosal inhibition) (14, 15, 16). In our study, rTMS applied over the right motor cortex might exert an influence on the contralateral left motor cortex through the mechanism of inter-hemispheric inhibition, which may secondarily affect the contralateral sensory cortex.

Because no significant change was found in P14 or N20 component, we considered that the change of N34 component occurred, not at the sensory pathway up to the primary sensory cortex, but through the interactions between sensory-motor cortices of both hemispheres. It was argued that the increased amplitude of an SEP component reflects inhibition rather than facilitation (7).

Seyal et al. (2005) already reported this contralateral effect on N20-P25, but did not investigate the effect of the ipsilateral sensory cortex. Our study is the first to show this contralateral SEP effects with no ipsilateral changes. Although the stimulation condition of rTMS used by Seyal et al. (2005) was a monophasic pulse of 0.3 Hz just as we used, their stimulation intensity was 10 % above the intensity of visual muscle contraction, being much stronger than ours (85 % of resting motor threshold) . The difference of intensity may mainly the reason of different influence on contralateral sensory cortex. We suspect the decreased amplitude by strong rTMS stimulation may relate with a kind of gating through contralateral motor cortex. On the other hand increased amplitude by weak rTMS stimulation in our result may originate mainly from contralateral sensory cortex probably through opposite mechanism of gating.

Left median nerve stimulation did not disclose any significant change of SEP components. The previous studies reported significant decrease of both N20a-P25 amplitude and P25-N33 amplitude (6) or no significant change (7). This difference may be due to the stimulation condition of rTMS. Urushihara's and our study used 0.2 Hz monophasic pulse whereas Enomoto's 1 Hz biphasic pulse. Recent study reported that phase was more important than frequency to induce SEP change (17).

Left median nerve stimulation did not disclose any significant change of SEPs, possibly because N34 amplitude on the left hemisphere was larger in the right rather than left median nerve stimulation and the finite change of N34 component on the left hemisphere was sensitively detected through right median nerve stimulation. It supports our result that sensory modification predominantly occurs on the contralateral side of rTMS.

In conclusion, monophasic very low-frequency rTMS over the motor cortex significantly increased the amplitude of N34

component generated on the contralateral hemisphere. Our results suggests that rTMS parameters used in this study could modify the cortical sensory processing predominantly on the contralateral hemisphere, possibly through the transcallosal pathways.

Reference

1. Pascal-Leone A, Valls-sole J, Brasil-Neto JP, Cammarota A, Hallett M: Effects of subthreshold repetitive transcranial motor cortex stimulation. Neurology 44: 892-898, 1994
2. Pascal-Leone A, Valls-sole J, Wassermann EM, Hallett M: Responses to rapid-rate transcranial magnetic stimulation of the human motor cortex. Brain 117: 847-858, 1994
3. Chen R, Classen J, Gerloff C, Celnik P, Wassermann EM, Cohen LG: Depression of motor cortex excitability by low-frequency transcranial magnetic stimulation. Neurology 48: 1398-1403, 1997.
4. Maeda F, Keenan JP, Tormos JM, Topka H, Pascual-Leone A: Modulation of corticospinal excitability by repetitive transcranial magnetic stimulation. Clinical Neurophysiology 111: 800-805, 2000
5. Fitzgerald PB, Fountain S, Daskalakis ZJ: A comprehensive review of the effects of rTMS on motor cortical excitability and inhibition. Clinical Neurophysiology 117: 2584-2596, 2006
6. Enomoto H, Ugawa Y, Hanajima R, Yuasa K, Mochizuki H, Terao Y, Shiio Y, Furubayashi T, Iwata NK, Kanazawa I: Decreased sensory cortical excitability after 1 Hz rTMS over the ipsilateral primary motor cortex. Clin Neurophysiol 112: 2154-2158, 2001
7. Urushihara R, Murase N, Rothwell J C, Harada M, Hosono Y, Asanuma K, Shimazu H, Nakamura K, Chikahisa S, Kitaoka K, Sei H, Morita Y, Kaji R: Effect of repetitive transcranial Magnetic stimulation applied over the premotor cortex on somatosensory-evoked potentials and regional cerebral blood flow. NeuroImage Jun 31: 699-709, 2006
8. Seyal M, Shatzel AJ, Richardson SP: Crossed inhibition of sensory cortex by 0.3Hz transcranial magnetic stimulation of motor cortex. J Clin Neurophysiol 22: 418-421, 2005
9. Murase N, Rothwell JC, Kaji R, Urushihara R, Nakamura K, Murayama N, Igasaki T, Sakata-Igasaki M, Mima T, Ikeda A, Shibasaki H: Subthreshold low-frequency repetitive transcranial magnetic stimulation over the premotor cortex modulates writer's cramp. Brain 128: 104-115, 2005
10. Oldfield RC: The assessment and analysis of handedness: The Edinburgh Inventry. Neuropsychologia 9: 97-114, 1971
11. Wassermann E M: Risk and safety of repetitive transcranial magnetic stimulation, Report and suggested guidelines from the International Workshop on the Safety of Repetitive Transcranial Magnetic Stimulation, June 5-7, 1996. Electroencephalogr Clin Neurophysiol 108: 1-16, 1998
12. Glio F, Rizzo V, Siebner HR, Rothwell JC: Effects on the right motor hand-area excitability produced by low-frequency rTMS over human contralateral homologous cortex. J Physiol 551: 563-573, 2003
13. Schambra HM, Sawaki L, Cohen LG: Moduration of excitability of human motor cortex (M1) by 1 Hz transcranial magnetic stimulation of the contralateral M1. Clin Neurophysiol 114: 130-133, 2003
14. Ferbert A, Caramia D, Priori A, Bertolasi L, Rothwell JC: Cortical projection to erector spinae muscles in man as assessed by focal transcranial magnetic stimulation. Electroencephalogr Clin Neurophysiol 85: 382-387, 1992
15. Boroojerdi B, Diefenbach K, Ferbert A: Transcallosal inhibition in cortical and subcortical cerebral vascular lesions. J Neurol Sci 144: 160-170, 1996
16. Murase N, Duque J, Mazzoccio R, Cohen LG: Influence of interhemispheric interactions on motor function in chronic stroke. Ann Neurol 55: 400-409, 2004
17. Hosono Y, Urushihara R, Harada M, Morita N, Murase N, Kunikane Y, Shimazu H, Asanuma K, Uguisu H, Kaji R: Comparison of monophasic versus biphasic stimulation in rTMS over premotor cortex: SEP and SPECT studies. Clin Neurophysiol 119: 2538-2545, 2008

Clinical Neurophysiology 120 (2009) 1143–1148

Contents lists available at ScienceDirect

Clinical Neurophysiology

journal homepage: www.elsevier.com/locate/clinph

Pre-movement gating of somatosensory-evoked potentials by self-initiated movements: The effects of ageing and its implication

Katsuya Ogata [a,*], Tsuyoshi Okamoto [b], Takao Yamasaki [a], Hiroshi Shigeto [a], Shozo Tobimatsu [a]

[a] Department of Clinical Neurophysiology, Neurological Institute, Graduate School of Medical Sciences, Kyushu University, 3-1-1 Maidashi, Higashi-Ku, Fukuoka 812-8582, Japan
[b] Department of Digital Medicine Initiative, Kyushu University, Fukuoka, Japan

ARTICLE INFO

Article history:
Accepted 22 January 2009
Available online 10 May 2009

Keywords:
Somatosensory-evoked potentials (SEPs)
Gating
Self-initiated movements
Pre-movements
Sensorimotor interaction

ABSTRACT

Objective: To study whether the gating effect of the self-initiated movements on the cortical somatosensory-evoked potentials (SEPs) is affected by ageing.
Methods: The SEPs elicited by stimulating the right median nerve were recorded in 14 young and 16 older healthy subjects, while self-initiated movements of the right fingers were performed at 5–10 s intervals. The amplitudes of the major components of the SEPs at F3 and C3′ (2 cm posterior to C3) during the pre-movement period were analysed as the resting condition subserving the baseline.
Results: The amplitudes at rest were significantly greater in the elderly than in the younger subjects. The amplitudes of P27, N35 and P45 at C3′ as well as N30 at F3 decreased significantly during the pre-movement period. However, the ratio of amplitudes in the pre-movement period to the resting period in the elderly was not significantly different from that in the younger subjects, except for the interaction of N30.
Conclusions: The effect of age on the gating of N30 at F3 may indicate an altered preparatory processing of self-initiated movement in the elderly. The gating effect of older subjects at C3′ is almost comparable to that of young ones, which appears to be a compensatory mechanism to maintain the precise movements.
Significance: Ageing affects the SEPs differently at rest and pre-movement gating.

1. Introduction

Sensorimotor integration is crucial for executing smooth voluntary movements in humans, and many studies have examined this by using evoked potentials. Sensory signals, for example, somatosensory-evoked potentials (SEPs) are modulated during active movements (Rushton et al., 1981; Cheron and Borenstein, 1987; Cohen and Starr, 1987; Tapia et al., 1987), and this modulation is called a gating phenomenon. As these studies evaluated gating during active movements, the concurrent inputs from nearby cortical areas probably interfered with the modulations by the sensory and motor areas which affect the activity of the sensory tracts.

The sensory information can also be modulated before movements by interactions with the activated motor areas. This is referred to as pre-movement gating (Shimazu et al., 1999); it is a process caused only by centrifugal processing without centripetal information. Therefore, understanding pre-movement gating is important to comprehend intra-cortical sensorimotor integration.

In our laboratory, we have used either externally triggered (ET) or self-initiated (SI) movements to study the functional connectivity amongst the motor-related cortical areas and the basal ganglia that are related to ET and SI tasks using functional magnetic resonance imaging (fMRI) (Taniwaki et al., 2003, 2006, 2007). In the ET tasks, warning signals were used to initiate movements, while in the SI tasks, the hands were moved at the subject's pace. Our results showed different activation patterns in the motor loops for SI and ET movements. The gating of the SEPs using an ET task revealed that N30, a main component at F3, was inhibited before the movements (Cohen and Starr, 1987; Murase et al., 2000). However, the tasks could involve recognition of the external signals and other mental processes rather than sensorimotor interactions. Therefore, additional information to understand sensorimotor integration can be obtained by evaluating SEP gating under the SI paradigm. Thus far, pre-movement gating in the upper-limb using an SI task has been evaluated by magneto-encephalography (MEG) (Wasaka et al., 2003, 2005, 2007) and SEPs (Legon et al., 2008) in young subjects. The strength of the dipole at P30m, but not at N20m or P60m, decreased significantly with MEG (Wasaka et al., 2003, 2005). Legon et al. (2008) reported that frontal N30 amplitude was significantly enhanced during the movement of the hand contralateral to the median nerve stimulation. However, there was no significant effect of either the ipsilateral or contralateral hand before movement.

We have found an age-related alteration of the functional interactions within the basal ganglia and cerebellar motor loop by fMRI

* Corresponding author. Tel.: +81 92 642 5543; fax: +81 92 642 5545.
E-mail address: katuya@med.kyushu-u.ac.jp (K. Ogata).

1388-2457/$36.00
doi:10.1016/j.clinph.2009.01.020

(Taniwaki et al., 2007). However, in the studies of SEP gating, little is known about the influence of ageing. Aging effect on the gating was augmented during voluntary isometric contraction (Touge et al., 1997); in their study, the enhanced gating could be attributed to both centripetal and centrifugal gatings. Thus, if the SI task is applied to pre-movement gating, the effect of ageing on the centrifugal gating can be determined more precisely.

Therefore, the aim of this study was to evaluate the effect of ageing on the pre-movement gating of SEPs under SI tasks.

2. Subjects and methods

2.1. Subjects

Thirty subjects (17 men and 13 women) with ages ranging from 20 to 75 years were studied. The subjects were divided into two groups: younger (age range: 20–38 years; nine men and five women) and older (age range: 60–75 years; eight men and eight women). All of them were right handed and none of them were receiving neurological medications or had had neurological disorders. A written informed consent was obtained from each subject after the nature of the experiment was fully explained. The experiments were approved by The Ethics Committee at Kyushu University.

2.2. SEP recordings

The subjects were seated on a comfortable reclining chair and were instructed to relax during the SEP measurements. Silver–silver chloride cup electrodes were attached to the scalp by collodion and filled with conductive jelly. The recording sites were F3, C3' (2 cm posterior to C3) and P3 according to the International 10–20 system, and the potentials at F3 and C3' were referred to the linked earlobes. The impedance of the electrodes was kept below 5 kΩ. The band-pass filter on the amplifier was set between 1 and 1000 Hz and the analysis time was from −10 to 90 ms. The sampling rate was 2.5 kHz.

The median nerve at the wrist was electrically stimulated with a stimulus duration of 0.2 ms. The intensity of the stimulus was adjusted to elicit mild twitches of the right thumb. The inter-stimulus intervals were randomised between 600 and 1000 ms (mean: 800 ms). All the data were stored in a personal computer using a signal processing software (Multiscope PSTH, Medical Try System, Tokyo, Japan) for offline analyses.

2.3. Experimental paradigm

In the previous studies, either finger extension (Murase et al., 2000; Wasaka et al., 2003, 2005) or flexion (Cohen and Starr, 1987; Tapia et al., 1987) was used while median nerve SEPs were recorded. To study the pre-movement gating of SEPs under SI tasks, we adopted the method of finger extension (Wasaka et al., 2003, 2005). The subjects were instructed to extend their index and middle fingers as quickly as possible and then relax. They were requested to move their fingers at their own pace every 5–10 s, and also to neglect the electrical stimuli at the wrist. They practised the movement for a short time. A pair of recording surface electrodes was attached 3 cm apart on the right extensor digitorum communis muscle to detect the finger extension. Surface electromyographs (EMGs) were recorded with a band-pass filter of 20–100 Hz. The low-pass filter was set at 100 Hz to discriminate the EMGs from the SEPs; thus, the artefacts of electric stimulation were mostly eliminated. The movement was repeated 500–600 times in one movement session. To detect finger extension, electroencephalograms (EEGs) and surface EMGs were recorded for 4–5 s each time the subjects moved their fingers from 3.5 to 4.5 s before the movement to 0.5 s after the detected EMGs. EEGs were also recorded in the resting condition for about 10 min for each subject. The EEGs under resting conditions were recorded both between and after the two movement sessions. The recordings of the first 2–3 min were used for averaging to make the number of epochs comparable to those of the movement sessions.

2.4. Data analyses

Trials contaminated with inappropriate movement were excluded from the analyses, and the beginning of finger extension was also adjusted by a visual inspection of the surface EMGs. The time period from −3000 to 0 ms of the finger movement was taken and divided into six segments of 500 ms for the analysis: between −3000 and −2500 ms, −2500 and −2000 ms, −2000 and −1500 ms, −2000 and −1500 ms, −1500 and −1000 ms, −1000 and −500 ms and −500 and 0 ms. For each segment, the EEGs were averaged to obtain the SEPs. The mean number of responses averaged for each bin ranged from 250 to 350. The peak-to-peak amplitudes of the SEP components were measured and compared amongst the different segments to evaluate the attenuation of the SEPs during the pre-movement period. The amplitudes of P22, N30 and P40 at F3, and N20, P27, N35 and P45 at C3' were analysed as the resting condition subserving the baseline.

The amplitude ratios were statistically analysed using two-way repeated measures analysis of variance (ANOVA). The within-subject factor was the time segment and the between-subject factor was the age group. The sphericity of the data was tested with Mauchly's test, and Greenhouse–Geisser-corrected significance values were used when sphericity was lacking. A post hoc analysis followed by Bonferroni's correction was used for multiple comparisons. The significance of the differences in the amplitudes at the resting condition between the two age groups was tested using the Student's t-tests. A $P < 0.05$ was considered to be significant.

3. Results

Several components are clearly visible in the grand-averaged SEPs at F3 and C3′ as shown in Fig. 1. In general, the amplitudes of the older subjects were greater than those of the younger subjects,

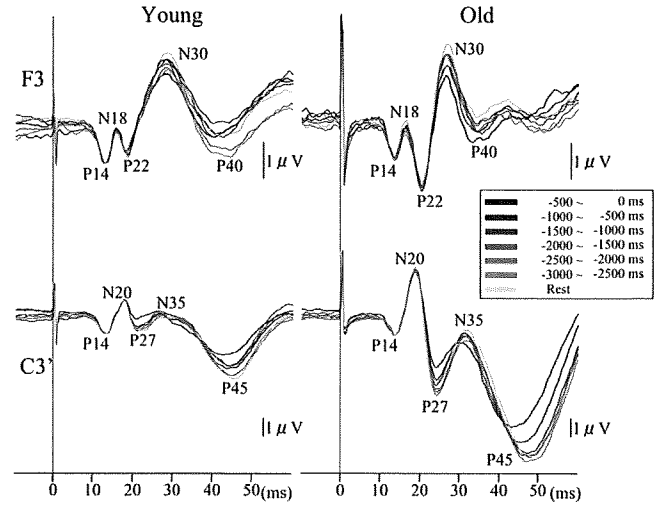

Fig. 1. Grand averaged waveforms of SEPs prior to movement and resting conditions for the younger ($n = 14$) and older ($n = 16$) subjects. Several components are identified at the F3 and C3′ electrodes. Although the amplitudes of the older subjects are generally larger than those of younger ones except for P14, the amplitudes of the late components become smaller as the time interval moves closer to the movement for both the groups.

Table 1
Amplitudes and latencies of the major components of SEPs in the resting condition.

	Amplitudes		Latencies	
	Young	Old	Young	Old
F3				
N18	1.28 ± 0.91	1.55 ± 0.55	16.40 ± 1.03	16.45 ± 0.84
P22	1.08 ± 0.10	2.25 ± 1.09*	18.94 ± 1.25	20.53 ± 0.82*
N30	3.41 ± 2.23	4.67 ± 2.46	28.26 ± 2.14	26.70 ± 1.04*
P40	3.01 ± 2.45	3.07 ± 1.87	39.69 ± 3.99	35.38 ± 3.45*
C3′				
N20	2.44 ± 1.58	4.49 ± 1.47*	17.97 ± 0.99	19.05 ± 0.73*
P27	2.59 ± 1.93	8.30 ± 3.91*	21.71 ± 1.63	24.68 ± 1.20*
N35	1.76 ± 1.25	4.86 ± 2.85*	29.69 ± 2.95	32.23 ± 2.86*
P45	4.14 ± 2.65	8.53 ± 4.27*	45.06 ± 2.65	47.65 ± 2.93*

* $P < 0.05$.

both in the resting condition and during the movements. In addition, the amplitudes of the SEPs were greatest in the resting condition and were gradually attenuated as the time interval was closer to the beginning of the finger movements in both the groups. These changes were observed at both F3 and C3′; however, the changes at C3′ were more prominent. At C3′, the amplitude of N20 did not change significantly, irrespective of the time segment; however, the later components were attenuated in the pre-movement period.

The amplitudes and latencies in the resting condition were compared between the two age groups using the Student's t-tests (Table 1). The amplitudes of P22 at F3 and N20, P27, N35 and P45 at C3′ in the elderly were significantly greater than those of the younger age group, while the amplitudes of N18, N30 and P40 at F3 were not significantly different. The latencies of the major components at rest were also significantly different between the two groups.

The ratios of the amplitudes between each time segment and resting condition were calculated to estimate the degree of attenuation at each time segment prior to the movement in the two age groups (Tables 2 and 3 and Fig. 2). When compared between the age groups, the ratios between the younger and older age groups were not significantly different except for an interaction between time and age for N30 at F3 ($P > 0.05$; ANOVA). The mean ratios of N30 decreased gradually for the elderly, while those for the younger subjects did not show such a trend (Fig. 2). To further confirm this finding, a *post hoc* analysis was carried out. As given in Table 3, there were significant differences for the older subjects between −500 and 0 ms and −3000 and −2500 ms and also between −500 and 0 ms and −2500 and −2000 ms. However, there was no significant difference for the younger subjects in any combination of the time periods.

There was a significant main effect for the time segment for P27, N35 and P45 at C3′ and for N30 at F3, which suggested that the peaks became smaller with a change in the time interval for both the younger and older age groups. A post hoc analysis also showed that P45 at C3′ and N30 at F3 were significantly different only between −500 and 0 ms and the rest of the segments, while P27 and N35 at C3′ had a much earlier gating. For P27, there was a significant difference between −1500 to −1000 ms and −3000 to −2500 ms, and between −1000 to −500 ms and −3000 to −2500 ms, as well as the difference between −500 to 0 ms and the rest. For N35, the segment between −1000 to −500 ms and −2500 to −2000 ms reached a significant level. In addition, the time window between −500 and 0 ms was also significant (Table 3).

4. Discussion

Our results showed that the amplitudes of the SEPs in the resting condition were significantly greater in the older subjects than in the younger ones. This is in agreement with the earlier reports (Lüders, 1970; Desmedt and Cheron, 1980, 1981). However, the effect of gating before the self-paced movements was almost the same for both the age groups except for N30 at F3, where the amplitude ratios normalised by the amplitudes at rest were used as the parameters. The gating effect of SEPs during the pre-movement period is probably caused by sensorimotor interactions and we suggest that this is related to the reduction of excessive afferent information (Lidsky et al., 1985). Our results imply that the function of sensorimotor interaction for the healthy older subjects was largely maintained in younger subjects.

We also suggest that there are different mechanisms involved in the amplitude reduction from the gating during movement preparation and the amplitude enhancement at rest due to ageing. Touge et al. (1997) reported that the gating effect was enhanced in older subjects during isometric contraction. In their study, the raw amplitudes, but not amplitude ratios, were used to evaluate the gating effect. It appears that the amplitude reduction should be evaluated as the ratio, that is, normalised by the amplitude of the resting condition because of the baseline differences caused by ageing.

The interaction between the two age groups and the time segment were evident for N30 at F3, which suggested that the reduction of the ratio in the pre-movement period was greater for the older subjects than for the younger ones. The mechanism for the differential gating effect due to ageing may reflect a higher function, such as cognition or motor imagery, rather than a motor preparation alone because N30 was depressed when a contingent negative variant (CNV) paradigm was used (Murase et al., 2000). Older subjects are reported to require more activated areas such as the pre-motor (PM) areas, cerebellum and pre-supplementary motor areas for voluntary movements (Wu and Hallett, 2005), and the connectivity of the basal ganglia–thalamocortical loop is reduced (Taniwaki et al., 2007). These age-related changes could contribute to the differential gating effect. In any case, our results suggest that the age of the subjects should be matched when the gating effect of N30 is assessed.

Apart from the difference in N30 at F3 between the age groups, there was a comparable gating effect of the peaks after N20 at C3′for both the groups. In SEP studies, there have been a few papers on the effect of pre-movement gating by upper-limb stimulation using SI tasks. Legon et al. (2008) reported a trend for pre-movement

Table 2
ANOVA table for the pre-movement gating.

Sites	Components	Time (main effect)	*P*	Time × age (interaction)	*P*
F3	P22	$F(3.663, 102.560) = 1.57$	0.192	$F(3.663, 102.560) = 0.799$	0.519
	N30	$F(3.302, 92.450) = 3.919$	0.009*	$F(3.302, 92.450) = 2.792$	0.040*
	P40	$F(3.317, 92.867) = 2.537$	0.056	$F(3.317, 92.867) = 0.732$	0.549
C3′	N20	$F(5, 140) = 0.409$	0.842	$F(5, 140) = 0.714$	0.614
	P27	$F(2.930, 82.045) = 22.107$	<0.001*	$F(2.930, 82.045) = 0.971$	0.409
	N35	$F(3.638, 101.861) = 17.725$	<0.001*	$F(3.638, 101.861) = 1.065$	0.374
	P45	$F(3.125, 87.493) = 14.848$	<0.001*	$F(3.125, 87.493) = 1.044$	0.379

* Indicates a statistically significant difference.

Table 3
Multiple comparisons for main effect (time) and interaction (time × age).

	−3000 to −2500 (ms)	−2500 to −2000 (ms)	−2000 to −1500 (ms)	−1500 to −1000 (ms)	−1000 to −500 (ms)	−500 to 0 (ms)
Main effect (time)[a]						
P27						
−3000 to −2500 (ms)		1.000	0.115	0.002*	0.007*	<0.001*
−2500 to −2000 (ms)			1.000	0.325	0.022*	<0.001*
−2000 to −1500 (ms)				1.000	0.945	<0.001*
−1500 to −1000 (ms)					1.000	<0.001*
−1000 to −500 (ms)						<0.001*
−500 to 0 (ms)						
N35						
−3000 to −2500 (ms)		1.000	1.000	0.363	0.606	<0.001*
−2500 to −2000 (ms)			1.000	0.484	0.024*	<0.001*
−2000 to −1500 (ms)				1.000	1.000	<0.001*
−1500 to −1000 (ms)					1.000	0.001*
−1000 to −500 (ms)						<0.001*
−500 to 0 (ms)						
P45						
−3000 to −2500 (ms)		1.000	0.839	1.000	0.234	0.001*
−2500 to −2000 (ms)			1.000	1.000	1.000	<0.001*
−2000 to −1500 (ms)				1.000	1.000	<0.001*
−1500 to −1000 (ms)					0.495	<0.001*
−1000 to −500 (ms)						<0.001*
−500 to 0 (ms)						
N30						
−3000 to −2500 (ms)		1.000	1.000	1.000	1.000	0.044*
−2500 to −2000 (ms)			1.000	1.000	1.000	0.039*
−2000 to −1500 (ms)				1.000	1.000	0.045*
−1500 to −1000 (ms)					1.000	0.008*
−1000 to −500 (ms)						0.092
−500 to 0 (ms)						
Interaction (time × age)[b]						
N30						
−3000 to −2500 (ms)		1.000	1.000	1.000	0.004*	0.013*
−2500 to −2000 (ms)			1.000	1.000	1.000	0.013*
−2000 to −1500 (ms)				1.000	1.000	0.550
−1500 to −1000 (ms)					0.606	0.043*
−1000 to −500 (ms)						1.000
−500 to 0 (ms)						

Matrix chart shows *P* values amongst each time window.
* Indicates significant differences between each pair. Note that P45 and N30 show a significant difference only between just before movement and the rest of the segments, while earlier gating starting at the period of −1500 to −1000 is evident for P27 and −1000 to −500 is evident for N35.
[a] *P* values were calculated from the data of both young and old subjects.
[b] *P* values were calculated from the old subjects only.

gating for N30 at F3 under the SI task, but not the peaks at C3′. The differences between our results and theirs probably resulted from the methodological differences: only young subjects participated in their study and they used the peak-to-peak amplitudes, but not the ratios, as a parameter. In addition, the stimulation rate used in our study was 0.8 Hz on an average, while it was 2 Hz in their study. This is important because it has been reported that increased stimulation rates reduce the amplitudes of the SEPs (Tomberg et al., 1989; Ibanez et al., 1995). Thus, the gating effect may have been reduced in their study by the higher stimulation rate (Touge et al., 1997).

In an MEG study, P30m of the SEFs was depressed during the SI pre-movement period, which is consistent with our results (Wasaka et al., 2003, 2005). The MEG results probably corresponded to the mild modulation of N30 at F3 and P27 at C3′ in this study because P30m is a tangential dipole of S1 (Wasaka et al., 2003), although N30 and P27 were attenuated to different degrees. P27 and N35 of the SEPs would partly include a radial component of SI (Allison et al., 1989), which would be difficult to detect with MEG. The differential gating of N30, P27 and N35 may imply that the gating effect in the primary sensorimotor areas can be different in different areas. Several investigators have suggested that N30 at F3 originated in area 3b (Allison et al., 1989; Sonoo et al., 1991). However, a case has been reported where N20 was impaired after a post-central lesion, while N30 was spared (Mauguière et al., 1983). Sleep has also been reported to lead to dissociated changes in the frontal and parietal SEPs (Noguchi et al., 1995). Although there is no consensus on the neural generators, our results may support the idea that N30 reflects a component generated beside S1. A recent review (Rossini et al., 2007) has suggested that physiological ageing is associated with more complex activations of the motor system to compensate the reduced motor skills. Older subjects have been shown to have enhanced activities in the motor-related areas (Wu and Hallett, 2005) and increased intra- and interhemispheric connectivity in the motor areas (Taniwaki et al., 2007). These findings are interpreted to be a compensatory increase of decreased motor performance. These compensatory activations can be partly responsible for the preserved gating effect in the elderly in our study.

Movement-related cortical potentials (MRCPs) appear before movement when SI tasks are used. The MRCPs consist mainly of 'Bereitschaftspotentials' (BPs) with a negative slope (NS). BPs are recorded from approximately −1500 ms, while NS is recorded approximately −500 ms. During the pre-movement period, the SEPs are decreased uniformly as early as −1500 to −500 ms; thus, the evolution of the MRCPs and SEP changes may be correlated.

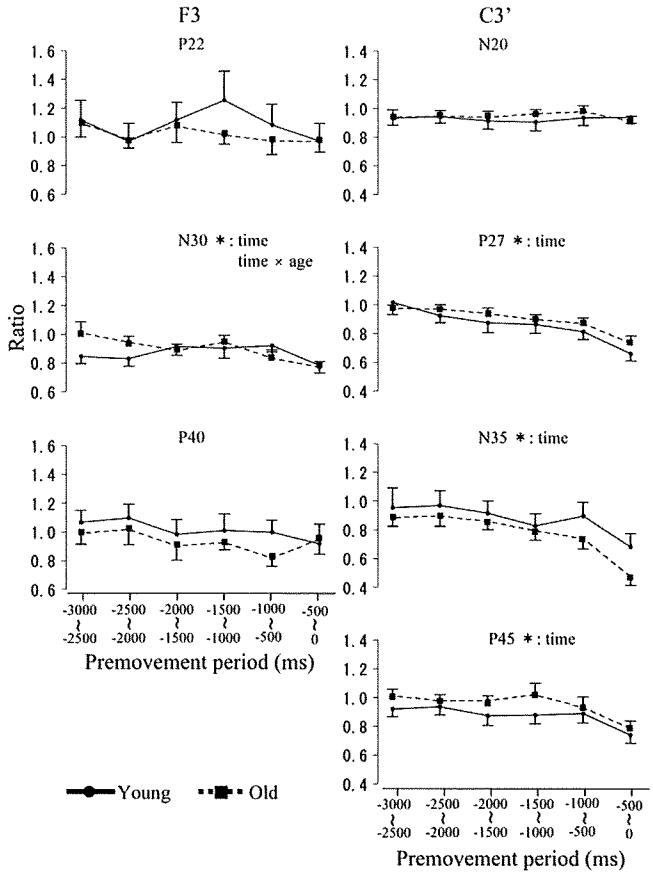

Fig. 2. Ratios of SEP amplitudes during pre-movement period compared to those during the resting condition. The ratios of P27, N35 and P45 at C3′ decrease during the pre-movement period, and N30 at F3 also decreases. There is a significant difference in the N30 ratio between the younger and older subjects at −3000 to −1500 ms. The error bars indicate standard error of the mean (SEM). $^{*}P < 0.05$, time: main effect of time segment, time × age: interaction of time segment and age groups.

The BPs are generated from the supplementary motor area (SMA) (Neshige et al., 1988), and an fMRI of SI tasks also showed activation of the SMA (Taniwaki et al., 2003, 2006). Thus, the SMA is a key structure for executing self-paced movements and may be related to the gating of SEPs. Matsunaga et al. (2004) reported that the SEPs at C3′ were enhanced after the sensorimotor area was activated by transcranial direct current stimulation. Similarly, inhibitory repetitive transcranial magnetic stimulation (TMS) on the primary motor area (M1) reduced the SEP amplitudes at C3′, while that of S1 and PM was unaffected (Enomoto et al., 2001). Conversely, our result showed that the activation of M1 in the pre-movement period resulted in an attenuation of the SEPs. Taken together, these findings indicate that the gating of SEPs cannot be simply explained by the direct effect of M1 activation on the SEPs.

The amplitude of N30 at F3 was selectively depressed during the pre-movement period when dual ET tasks were employed (Murase et al., 2000). The dual ET tasks refer to tasks that have two signals of warning and starting movement (Shimazu et al., 1999; Murase et al., 2000). CNVs are recorded at the central leads during these tasks, which reflect the functions of the prefrontal, PM, SMA and the primary sensorimotor areas (Gemba et al., 1990; Hamano et al., 1997). Thus, these areas may contribute to the attenuation of N30 under dual ET tasks. Gating with mental motor simulation (MMS) is reflected in N30 of the frontal leads, but not in P27 of the central leads, as that with dual ET tasks (Cheron and Borenstein, 1992). MMS requires motor images and activates PM, SMA and M1 (Roland et al., 1980; Decety and Grezes, 2006). Therefore, it probably shares PM activation and other cognitive process with dual ET tasks, which may explain the gating of N30 by MMS and dual ET tasks. In contrast, under a single ET task that uses one signal to start the movements, the pre-movement gatings showed that P27 at the central leads was attenuated (Starr and Cohen, 1985) at approximately 100 ms before the movement, although N30 was not recorded. As the period after the signal in a single ET task would include the process of movement initiation, the SEP gating of a single ET task may share a common mechanism of gating with that of the SI task.

In summary, the amplitudes of the SEPs at rest were significantly greater in the elderly than in younger subjects. However, the degree of the gating effect during the pre-movement period was almost the same for both the younger and older groups, except for N30 at F3. The mechanism of the pre-movement gating under SI conditions is probably due to an attenuation of S1 activity, and SMA should be an important structure that underlies the pre-movement gating. The larger SEP amplitudes at rest could be related to enhanced activities in the motor-related areas with increasing intra- and inter-hemispheric connectivity in the elderly. This may result in the preservation of gating. Therefore, pre-movement gating under the SI task can be useful for the investigation of centrifugal processing of motor function. However, care should be taken when this technique is applied to the movement disorders because of the ageing effect.

Financial interests

None.

Acknowledgements

The authors are grateful to Dr. Duco I. Hamasaki for reading the entire text and making a number of helpful suggestions. This study was supported by Grant-in-Aid for Scientific Research (C) from the Ministry of Education, Culture, Sports, Science and Technology, Japan. It was also supported by Aihara Complexity Modeling Project, ERATO, JST.

References

Allison T, McCarthy G, Wood CC, Darcey TM, Spencer DD, Williamson PD. Human cortical potentials evoked by stimulation of the median nerve. I. Cytoarchitectonic areas generating short-latency activity. J Neurophysiol 1989;62:694–710.

Cheron G, Borenstein S. Specific gating of the early somatosensory evoked potentials during active movement. Electroencephalogr Clin Neurophysiol 1987;67:537–48.

Cheron G, Borenstein S. Mental movement simulation affects the N30 frontal component of the somatosensory evoked potential. Electroencephalogr Clin Neurophysiol 1992;84:288–92.

Cohen LG, Starr A. Localization, timing and specificity of gating of somatosensory evoked potentials during active movement in man. Brain 1987;110:451–67.

Decety J, Grezes J. The power of simulation: imagining one's own and other's behavior. Brain Res 2006;1079:4–14.

Desmedt JE, Cheron G. Somatosensory evoked potentials to finger stimulation in healthy octogenarians and in young adults: wave forms, scalp topography and transit times of parietal and frontal components. Electroencephalogr Clin Neurophysiol 1980;50:404–25.

Desmedt JE, Cheron G. Non-cephalic reference recording of early somatosensory potentials to finger stimulation in adult or aging normal man: differentiation of widespread N18 and contralateral N20 from the prerolandic P22 and N30 components. Electroencephalogr Clin Neurophysiol 1981;52:553–70.

Enomoto H, Ugawa Y, Hanajima R, Yuasa K, Mochizuki H, Terao Y, et al. Decreased sensory cortical excitability after 1 Hz rTMS over the ipsilateral primary motor cortex. Clin Neurophysiol 2001;112:2154–8.

Gemba H, Sasaki K, Tsujimoto T. Cortical field potentials associated with hand movements triggered by warning and imperative stimuli in the monkey. Neurosci Lett 1990;113:275–80.

Hamano T, Luders HO, Ikeda A, Collura TF, Comair YG, Shibasaki H. The cortical generators of the contingent negative variation in humans: a study with subdural electrodes. Electroencephalogr Clin Neurophysiol 1997;104:257–68.

Ibanez V, Deiber MP, Sadato N, Toro C, Grissom J, Woods RP, et al. Effects of stimulus rate on regional cerebral blood flow after median nerve stimulation. Brain 1995;118:1339–51.
Legon W, Meehan SK, Staines WR. The relationship between frontal somatosensory-evoked potentials and motor planning. Neuroreport 2008;19:87–91.
Lidsky TI, Manetto C, Schneider JS. A consideration of sensory factors involved in motor functions of the basal ganglia. Brain Res Rev 1985;9:133–46.
Lüders H. The effect of aging on the wave form of the somatosensory cortical evoked potential. Electroencephalogr Clin Neurophysiol 1970;29:450–60.
Matsunaga K, Nitsche MA, Tsuji S, Rothwell JC. Effect of transcranial DC sensorimotor cortex stimulation on somatosensory evoked potentials in humans. Clin Neurophysiol 2004;115:456–60.
Mauguière F, Desmedt JE, Courjon J. Astereognosis and dissociated loss of frontal or parietal components of somatosensory evoked potentials in hemispheric lesions. Detailed correlations with clinical signs and computerized tomographic scanning. Brain 1983;106:271–311.
Murase N, Kaji R, Shimazu H, Katayama-Hirota M, Ikeda A, Kohara N, et al. Abnormal premovement gating of somatosensory input in writer's cramp. Brain 2000;123:1813–29.
Neshige R, Luders H, Shibasaki H. Recording of movement-related potentials from scalp and cortex in man. Brain 1988;111:719–36.
Noguchi Y, Yamada T, Yeh M, Matsubara M, Kokubun Y, Kawada J, et al. Dissociated changes of frontal and parietal somatosensory evoked potentials in sleep. Neurology 1995;45:154–60.
Roland PE, Larsen B, Lassen NA, Skinhoj E. Supplementary motor area and other cortical areas in organization of voluntary movements in man. J Neurophysiol 1980;43:118–36.
Rossini PM, Rossi S, Babiloni C, Polich J. Clinical neurophysiology of aging brain: from normal aging to neurodegeneration. Prog Neurobiol 2007;83:375–400.
Rushton DN, Rothwell JC, Craggs MD. Gating of somatosensory evoked potentials during different kinds of movement in man. Brain 1981;104:465–91.
Shimazu H, Kaji R, Murase N, Kohara N, Ikeda A, Shibasaki H, et al. Pre-movement gating of short-latency somatosensory evoked potentials. Neuroreport 1999;10:2457–60.
Sonoo M, Shimpo T, Takeda K, Genba K, Nakano I, Mannen T. SEPs in two patients with localized lesions of the postcentral gyrus. Electroencephalogr Clin Neurophysiol 1991;80:536–46.
Starr A, Cohen LG. 'Gating' of somatosensory evoked potentials begins before the onset of voluntary movement in man. Brain Res 1985;348:183–6.
Taniwaki T, Okayama A, Yoshiura T, Nakamura Y, Goto Y, Kira J, et al. Reappraisal of the motor role of basal ganglia: a functional magnetic resonance image study. J Neurosci 2003;23:3432–8.
Taniwaki T, Okayama A, Yoshiura T, Togao O, Nakamura Y, Yamasaki T, et al. Functional network of the basal ganglia and cerebellar motor loops in vivo: different activation patterns between self-initiated and externally triggered movements. Neuroimage 2006;31:745–53.
Taniwaki T, Okayama A, Yoshiura T, Togao O, Nakamura Y, Yamasaki T, et al. Age-related alterations of the functional interactions within the basal ganglia and cerebellar motor loops in vivo. Neuroimage 2007;36:1263–76.
Tapia MC, Cohen LG, Starr A. Selectivity of attenuation (i.e., gating) of somatosensory potentials during voluntary movement in humans. Electroencephalogr Clin Neurophysiol 1987;68:226–30.
Tomberg C, Desmedt JE, Ozaki I, Nguyen TH, Chalklin V. Mapping somatosensory evoked potentials to finger stimulation at intervals of 450 to 4000 msec and the issue of habituation when assessing early cognitive components. Electroencephalogr Clin Neurophysiol 1989;74:347–58.
Touge T, Takeuchi H, Sasaki I, Deguchi K, Ichihara N. Enhanced amplitude reduction of somatosensory evoked potentials by voluntary movement in the elderly. Electroencephalogr Clin Neurophysiol 1997;104:108–14.
Wasaka T, Hoshiyama M, Nakata H, Nishihira Y, Kakigi R. Gating of somatosensory evoked magnetic fields during the preparatory period of self-initiated finger movement. Neuroimage 2003;20:1830–8.
Wasaka T, Nakata H, Akatsuka K, Kida T, Inui K, Kakigi R. Differential modulation in human primary and secondary somatosensory cortices during the preparatory period of self-initiated finger movement. Eur J Neurosci 2005;22:1239–47.
Wasaka T, Kida T, Nakata H, Akatsuka K, Kakigi R. Characteristics of sensori-motor interaction in the primary and secondary somatosensory cortices in humans: a magnetoencephalography study. Neuroscience 2007;149:446–56.
Wu T, Hallett M. The influence of normal human ageing on automatic movements. J Physiol 2005;562:605–15.

Journal of the Neurological Sciences 281 (2009) 34–40

Contents lists available at ScienceDirect

Journal of the Neurological Sciences

journal homepage: www.elsevier.com/locate/jns

Multimodality-evoked potential study of anti-aquaporin-4 antibody-positive and -negative multiple sclerosis patients

Akihiro Watanabe [a,1], Takuya Matsushita [a,1], Hikaru Doi [a], Takashi Matsuoka [a], Hiroshi Shigeto [a,b], Noriko Isobe [a], Yuji Kawano [a], Shozo Tobimatsu [b], Jun-ichi Kira [a,*]

[a] Department of Neurology, Neurological Institute, Graduate School of Medical Sciences, Kyushu University, Japan
[b] Department of Clinical Neurophysiology, Neurological Institute, Graduate School of Medical Sciences, Kyushu University, Japan

ARTICLE INFO

Article history:
Received 22 July 2008
Received in revised form 7 January 2009
Accepted 25 February 2009
Available online 1 April 2009

Keywords:
Anti-aquaporin-4 antibody
Multiple sclerosis
Neuromyelitis optica
Opticospinal form
Visual-evoked potential
Sensory evoked potential
Motor evoked potential

ABSTRACT

Neuromyelitis optica (NMO) is claimed to be a distinct disease entity from multiple sclerosis (MS) because of its strong association with NMO-IgG/anti-AQP4 antibody; however, the in vivo role of the antibody remains unknown. Therefore, we aimed to clarify whether the presence of anti-AQP4 antibody is associated with any abnormalities in multimodality-evoked potentials in 111 patients with relapsing–remitting or relapsing-progressive MS, including the opticospinal form of MS, 18 of whom were seropositive for anti-AQP4 antibody. More patients with anti-AQP4 antibody showed a lack of the P100 component on visual-evoked potentials (VEPs) than those without the antibody (11/17, 64.7% vs. 20/84, 23.8%, $p=0.003$), whereas the frequency of delayed P100 latency was significantly higher in the latter group than in the former (1/17, 5.9% vs. 28/84, 33.3%, $p=0.021$). The frequencies of non-responses and delayed central sensory conduction times in median and posterior tibial nerve somatosensory-evoked potentials (SEPs) were not significantly different between anti-AQP4 antibody-positive and -negative patients. In terms of upper and lower limb motor-evoked potentials (MEPs), the frequencies of non-responses and delayed central motor conduction times did not differ significantly based on the presence or absence of anti-AQP4 antibody. The frequency of optic nerve lesions on MRI was significantly higher in anti-AQP4 antibody-positive patients than in anti-AQP4 antibody-negative patients ($p=0.0137$). Multiple logistic analyses revealed that anti-AQP4 antibody positivity (OR = 8.406, $p=0.02$) and unevoked VEP responses (OR = 35.432, $p<0.001$) were significantly related to development of severe visual impairment. Such an association of anti-AQP4 antibody with disability was not found for either severe motor or sensory impairment. These findings suggest a distinctive nature of optic nerve lesions between anti-AQP4 antibody-positive and -negative patients; lesions are supposed to be more necrotic in the former group and more demyelinating in the latter.

1. Introduction

Multiple sclerosis (MS) is an inflammatory demyelinating disease of the central nervous system (CNS) that is generally considered to be mediated by myelin-autoreactive T cells. In Asians, selective and severe involvement of the optic nerves and spinal cord is characteristic [1]. There are two distinct subtypes of MS: the opticospinal form (OSMS), which has similar features to the relapsing–remitting form of neuromyelitis optica (NMO) in Western populations [2–5], and the conventional form (CMS), which is similar to classical MS in Western populations [1,2,6,7].

Recently, a specific IgG expressed by NMO patients, designated NMO-IgG, was described [8]; its relevant antigen was reported to be aquaporin-4 (AQP4) [9]. Because of the high specificity of NMO-IgG/anti-AQP4 antibody, NMO has been claimed to be a distinct disease entity with a fundamentally different causal mechanism from MS [10]. In a selected series of Japanese patients with OSMS, Nakashima et al. [11] reported an NMO-IgG positivity rate of approximately 60%, and we and others found that anti-AQP4 antibody is present in about 40 to 60% of OSMS patients [12]. Thus OSMS has now been suggested to be the same disease as NMO [13]. Additionally, selective loss of AQP4 from acute lesions in autopsied OSMS spinal cord specimens has been described [14,15]. Therefore, it is hypothesized that anti-AQP4 antibody is a causative agent for both NMO and OSMS and that demyelination is secondarily produced following damage to the astrocyte foot process, where AQP4 is localized [14–16].

Longitudinally extensive spinal cord lesions (LESCLs) extending over three or more vertebral segments [3,10] are considered to be characteristic of NMO; however, in Asians, LESCLs are observed in one-

* Corresponding author. Department of Neurology, Neurological Institute, Graduate School of Medical Sciences, Kyushu University, 3-1-1 Maidashi, Higashi-ku, Fukuoka 812-8582, Japan. Tel.: +81 92 642 5340; fax: +81 92 642 5352.
E-mail address: kira@neuro.med.kyushu-u.ac.jp (J. Kira).
[1] These authors contributed equally to this work.

0022-510X/$ – see front matter © 2009 Elsevier B.V. All rights reserved.
doi:10.1016/j.jns.2009.02.371

fourth of CMS patients [2,17–20], reflecting the severe spinal cord damage commonly seen in Asians. In addition, diffused spinal cord lesions were found in 13% of individuals in a Western MS series published recently [21]. These observations render delineation between MS and NMO on the basis of MRI findings to be difficult, especially in Asians.

We previously reported that, according to multiple logistic analyses, only relapse rates, but neither the presence of LESCLs nor EDSS scores, were associated with the presence of anti-AQP4 antibody [12]. Nakashima et al. [11] reported that only severe visual impairment was significantly associated with the presence of NMO-IgG. On the other hand, NMO-IgG was detected in 9% of Western MS patients [8] and 15% of Japanese classical MS patients [11], whereas 30 to 50% of NMO patients or OSMS patients with LESCLs are consistently negative for NMO-IgG/anti-AQP4 antibody [8,11,12,22]. Thus the in vivo role of NMO-IgG or anti-AQP4 antibodies in NMO lesion formation is currently uncertain. Therefore, it is critical to disclose which clinical parameters are associated with NMO-IgG/anti-AQP4 antibody in order to clarify the in vivo role of these antibodies. Multimodality-evoked potentials, including visual-evoked potentials (VEPs), somatosensory-evoked potentials (SEPs) and motor-evoked potentials (MEPs), are useful tools for detecting both clinically overt and silent lesions in the optic nerves and spinal cord. Therefore, in the present study, we first aimed to clarify whether the presence of anti-AQP4 antibody is associated with any abnormalities in evoked potentials (EPs) in a series of MS patients with and without anti-AQP4 antibody. Second, we studied the relationships of the presence of MRI lesions in the optic nerve pathway and the spinal cord with both EP abnormalities and anti-AQP4 antibody status. Finally, we performed multiple logistic analyses to disclose possible factors contributing to the development of severe visual, sensory and motor impairment.

2. Patients and methods

2.1. Patients

One hundred and eleven consecutive patients who were diagnosed with clinically definite MS according to the criteria of Poser et al. [23] at the MS clinic in the Department of Neurology, Kyushu University Hospital, and subjected to both multimodality-evoked potential study and anti-AQP4 antibody assay, during the period 1987–2007, were enrolled in the present study. All patients underwent a thorough neurological examination and routine laboratory tests. All were followed-up and clinically evaluated at regular intervals in the MS clinic. Their medical and EP records were analyzed retrospectively in the present study. None of the patients were seropositive for human T-cell leukemia virus type I. All patients had a relapsing–remitting or relapsing-progressive course, and no patients with primary progressive MS were included in the present study. Patients with monophasic NMO without subsequent relapse were also excluded to avoid including patients with acute disseminated encephalomyelitis.

The disability status of the patients was scored according to the Expanded Disability Status Scale (EDSS) of Kurtzke [24]. Visual acuity was evaluated as: 0, normal; −1, mild visual impairment; −2, finger counting; −3, light perception; −4, total blindness. Muscle power was evaluated as; 0, normal; −1, mild weakness; −2, moderate weakness, −3, severe weakness; −4, complete paralysis. Superficial sensation was evaluated as: 10, normal; 9 to 1, mild to severe; 0, loss while vibration and position sensation were evaluated as: 0, normal; −1, mild impairment; −2, moderate; −3, severe; −4, loss.

2.2. Anti-AQP4 antibody assay

Anti-AQP4 antibody was assayed by an immunofluorescence method described previously [12]. Briefly, a full-length cDNA encoding human AQP4 (AQP4 transcript variant a; GenBank accession number NM_001650) was amplified from a cDNA library generated from commercially obtained human spinal cord mRNAs (Clontech, Mountain View, CA, USA). The PCR product was cloned into the pDONR221 vector (Invitrogen, Carlsbad, CA, USA), and its sequence was confirmed. After sequencing, the AQP4 cDNA was transferred to the pcDNA-DEST53 expression vector (Invitrogen). Human embryonic kidney HEK-293 cells maintained in Dulbecco's modified Eagle's medium (DMEM) containing 10% fetal calf serum were seeded at 10,000 cells/well onto 8-well chamber slides (Becton Dickinson, Franklin Lakes, NJ, USA) 24 h before transfection. The cells were transfected with 100 ng/well of the GFP-AQP4 fusion protein expression vector using the FuGENE6 Transfection Reagent (Roche, Basel, Switzerland) according to the manufacturer's instructions. At 48 h after transfection, the cells were initially incubated with the human sample serum diluted 1:4 with DMEM for 1 h at 37.0 °C to avoid permeabilization during fixation, washed in phosphate-buffered saline and visualized with an Alexa 594-conjugated goat anti-human IgG antibody (Invitrogen). Fluorescence was observed using a confocal laser-scanning microscope (Flu FV300; Olympus Optical Co., Tokyo, Japan). With the examiners blinded to the origin of the specimens, the anti-AQP4 antibody assay was carried out at least twice for each sample, and those that gave a positive result twice were deemed to be positive.

2.3. Evoked potentials

A checkerboard pattern was back-projected onto a translucent screen. Stimulation was phase reversed at 1 Hz. The stimulating field subtended 8 deg in diameter and the check size was 30 min of arc. The mean luminance was 180 cd/m^2 with a contrast level of 90%. Subjects were instructed to fixate their eyes at the center of the stimulus field at a viewing distance of 100 cm. Monocular full visual fields were stimulated. VEPs were recorded from an electrode placed at Oz with a reference at Fz (International 10–20 system). A total of 100 responses were averaged and repeated at least twice to establish reproducibility. The latency of the major positive peak (P100) was measured [25].

SEPs were obtained by stimulating the median nerve at the wrist and the posterior tibial nerve at the ankle with frequencies of 5 Hz and 2 Hz, respectively. Recording electrodes for upper limbs were placed over Erb's point, the seventh cervical vertebra, and C3′ or C4′ over the somatosensory cortex. For the lower limbs, the electrodes were placed over the 12th thoracic vertebra and Cz′. Fz was used as the reference for all electrodes. A total of 500 responses for the upper limbs and 350 responses for the lower limbs were averaged and repeated at least twice to establish reproducibility. The peak latencies of the responses were measured: N9 (Erb), N13 (C7) and N20 (sensory cortex) for median nerve SEPs and N20 (Th12) and P37 (sensory cortex) for tibial nerve SEPs. The central sensory conduction time (CSCT) was calculated as N20-N13 for the upper limbs and P37-N20 for the lower limbs [26].

MEPs were obtained from the abductor pollicis brevis for the upper limbs and the abductor hallucis for the lower limbs. Magnetic stimuli were applied to the motor cortex and the seventh cervical vertebra (C7) using a figure-of-eight-shaped coil for the upper extremities, while a double-cone coil was used to stimulate the motor cortex for the lower extremities, and the fourth lumbar root (L4) was elicited by the figure-of-eight-shaped coil. We assessed MEP latencies, and the central motor conduction time (CMCT) was calculated as the difference between cortical motor latency and peripheral motor latency [26].

The upper normal limits (mean + 3 SD, ms) of EPs in our laboratory were as follows; VEP P100, 121.0; CSCT of the median nerve SEP, 7.33; CSCT of the posterior tibial nerve SEP, 21.83; CMCT of the upper limb MEP, 10.67; CMCT of the lower limb MEP, 21.04.

Table 1
Demographic features of MS patients in the present study.

	Anti-AQP4 antibody-positive patients ($n=18$)	Anti-AQP4 antibody-negative patients ($n=93$)
Male/female	0/18*	32/61
Age at onset (years)[a]	39.3 ± 14.5*	31.5 ± 12.7
Disease duration (years)[a]	12.6 ± 7.0	11.0 ± 9.2
Annualized relapse rate[a]	1.1 ± 0.7*	0.7 ± 0.6
LESCLs on MRI	13/18 (72.2%)*	36/93 (38.7%)
Optic nerve lesions on MRI[b]	7/34 (20.6%)*	10/162 (6.2%)
EDSS scores at the last examination[a]	5.0 ± 2.5	4.0 ± 2.8

AQP4 = aquaporin-4; EDSS = Expanded Disability Status Scale of Kurtzke; LESCLs = longitudinally extensive spinal cord lesions extending three or more vertebral segments.
*$p<0.05$ in comparison between patients with and without anti-AQP4 antibody.
[a] Mean ± SD.
[b] Each eye (each optic nerve) was examined.

Recording results were divided into three groups according to P100 latency, CSCT and CMCT: the normal group had normal latency, the unevoked group had a lack of cortical responses, at least on one side of the eye or body, and the delayed group had prolonged latency on at least one side.

2.4. Magnetic resonance imaging

All MRI studies were performed using Magnetom Vision and Symphony 1.5-T units (Siemens Medical Systems, Erlangen, Germany), as previously described [12]. We obtained 98 MRI samples from patients who underwent VEP study, 81 from those who were subjected to SEP study, and 86 from those who underwent MEP study. Lesions visible on T2 and FLAIR images were counted.

2.5. Statistical analyses

The frequencies of given observations between anti-AQP4 antibody-positive and -negative patients were compared by Fisher's exact test. Values not normally distributed (age, duration, rate, or scoring) were compared by the Mann–Whitney U test. When multiple comparisons were made, uncorrected p values were corrected by the number of comparisons to calculated corrected p values (Bonferroni–Dunn's correction). Multiple logistic analyses were performed to assess possible factors contributing to development of severe visual impairment (finger counting or worse), severe muscle weakness (moderate weakness or worse) in lower limbs and severe sensory impairment (moderate or more severe position sense impairment) in lower limbs. The variables studied were gender, age at onset, disease duration from onset to time of study, anti-AQP4 antibody status, presence or absence of MRI lesions in the optic nerve pathway or spinal cord, unevoked EP records, corticosteroid treatment at study, plasma exchange at study, and interferon (IFN) beta therapy at time of study. In all assays, statistical significance was set at $p<0.05$.

3. Results

3.1. Demographic features

The demographic features of the patients are summarized in Table 1. Patients with anti-AQP4 antibody showed a significantly higher frequency of females ($p=0.001$), higher age at onset ($p=0.030$), higher annual relapse rates ($p=0.006$), and higher frequency of LESCLs ($p=0.011$) and optic nerve lesions ($p=0.0137$) compared with those without anti-AQP4 antibody, while disease duration was similar between the two groups. The latest EDSS scores were higher in patients with anti-AQP4 antibody than those without the antibody, but the differences were not significant.

3.2. Visual function and VEP findings

The visual functions and VEP findings of the patients are summarized in Table 2. Past and present history of visual impairment at the time of VEP study and the frequency of patients with severe visual impairment (finger counting or worse) were significantly higher among patients with anti-AQP4 antibody than those without the antibody ($p=0.048$ and $p=0.001$, respectively). The visual acuity of anti-AQP4 antibody-positive patients was significantly worse than that of those without the antibody ($p=0.001$). The frequencies of optic atrophy and/or temporal pallor were also higher in anti-AQP4 antibody-positive patients than anti-AQP4 antibody-negative patients, but the difference was not significant. Frequencies of immunotherapies, such as IFN beta, corticosteroid, and plasma exchange, at the time of study, were not significantly different between anti-AQP4 antibody-positive patients and anti-AQP4 antibody-negative patients. P100 was not elicited in 11 of the 17 (64.7%) patients with anti-AQP4 antibody and 20 of the 84 (23.8%) patients without the antibody, while P100 was delayed in one (5.9%) patient with anti-AQP4 antibody and 28 (33.3%) patients without the antibody. As a result, significantly more patients with anti-AQP4 antibody showed a lack of the P100 component than did patients without the antibody ($p=0.003$), whereas the frequency of delayed P100 latency was significantly higher in the latter group than in the former ($p=0.021$). VEP results from each eye were also compared. The frequency of eyes showing a lack of the P100 component was significantly higher among patients with the anti-AQP4 antibody (38.2%) than among those without the antibody (15.1%) ($p=0.003$), whereas the frequency of delayed P100 latency was significantly higher in the latter group (30.1%) than in the former (11.8%) ($p=0.033$) (Fig. 1). VEP findings in the remission phase also showed essentially the same results. The frequency of patients in remission showing a lack of the P100 component was significantly higher among anti-AQP4 antibody-positive patients (69.2%) than among those

Table 2
Visual function and VEP findings in MS patients with and without anti-AQP4 antibody.

		Anti-AQP4 antibody-positive patients ($n=17$)	Anti-AQP4 antibody-negative patients ($n=84$)
Age at time of VEP study (years)[a]		44.7 ± 14.4	39.2 ± 11.9
Age at onset (years)[a]		39.3 ± 14.5*	31.5 ± 12.7
Time elapsed from disease onset to VEP study (years)[a]		6.6 ± 6.8	7.1 ± 8.3
Past and present history of visual impairment at time of VEP study		15/17 (88.2%)*	51/84 (60.7%)
Severe visual impairment (finger counting or worse)		9/17 (52.9%)*	11/84 (13.1%)
Visual acuity[ab]		−1.8 ± 1.6*	−0.6 ± 0.9
Optic atrophy/temporal pallor		8/17 (47.1%)	22/84 (26.2%)
Remission phase percentage at VEP study		13/17 (76.5%)	44/84 (52.4%)
IFN beta therapy at time of VEP study		5/17 (29.4%)	17/84 (20.2%)
Corticosteroid therapy at time of VEP study		14//17 (82.4%)	54/84 (64.3%)
Plasma exchange at time of VEP study		0/17 (0.0%)	3/84 (3.6%)
VEP (P 100)	Unevoked	11/17* (64.7%)	20/84 (23.8%)
	Delayed	1/17* (5.9%)	28/84 (33.3%)
	Normal	5/17 (29.4%)	36/84 (42.9%)

AQP4 = aquaporin-4; IFNβ = interferon β; VEP = visual-evoked potentials.
*$p<0.05$ in comparison between patients with and without anti-AQP4 antibody.
[a] Mean ± SD.
[b] Visual acuity was scored as follows: 0, normal; −1, mild vision impairment; −2, finger counting; −3, light perception; −4, total blindness.

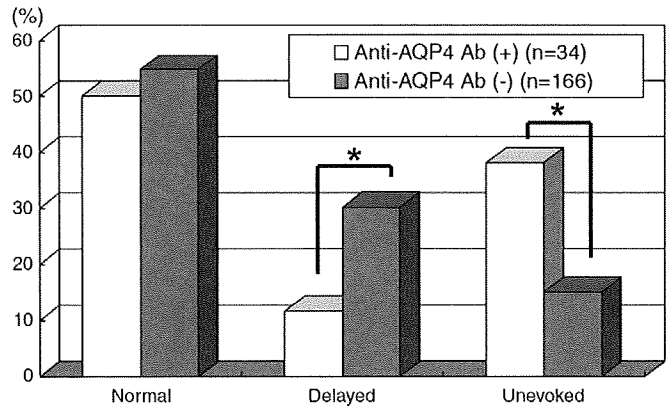

Fig. 1. Results of the VEP study in each eye. *$p<0.05$ in comparison between anti-AQP4 antibody-positive and -negative eyes.

without the antibody (33.3%) ($p=0.028$), whereas the frequency of delayed P100 latency was higher in the latter group (33.3%) than in the former (7.7%), but without statistical significance ($p=0.087$).

3.3. Sensory function and SEP findings

The sensory functions and SEP findings of our patients are summarized in Table 3. Age at SEP examination was higher in anti-AQP4 antibody-positive patients than in anti-AQP4 antibody-negative patients ($p=0.020$). Sensory impairment in upper and lower limbs was not different significantly between patients with and without anti-AQP4 antibody who were subjected to SEP studies. Frequencies of immunotherapies, such as IFN beta, corticosteroid, and plasma exchange, at the time of study, were not significantly different between anti-AQP4 antibody-positive patients and anti-AQP4 antibody-negative patients. A lack of an evoked response in the median nerve SEPs was observed in none of 12 patients with anti-AQP4 antibody and 10 of 60 (16.7%) patients without anti-AQP4 antibody, while a delayed CSCT was found in two of 12 (16.7%) patients with anti-AQP4 antibody and eight of 60 (13.3%) patients without anti-AQP4 antibody. Regarding posterior tibial nerve SEPs, one of 12 (8.3%) patients with anti-AQP4 antibody and 11 of 60 (18.3%) patients without the antibody showed a lack of evoked responses, while two of 12 (16.7%) patients with anti-AQP4 antibody and 16 of 60 (26.7%) patients without the antibody showed delayed CSCTs. There was no significant difference in the frequencies of abnormal findings between anti-AQP4 antibody-positive and -negative patients.

Table 3
Sensory functions and SEP findings of MS patients with and without anti-AQP4 antibody.

		Anti-AQP4 antibody - positive patients ($n=12$)	Anti-AQP4 antibody - negative patients ($n=60$)
Age at time of SEP study (years)[a]		49.5 ± 13.4*	39.4 ± 12.3
Time elapsed from disease onset to SEP study (years)[a]		6.8 ± 6.8	8.0 ± 10.3
Past and present history of sensory impairment at time of SEP study		11/12 (91.7%)	54/60 (90.0%)
Superficial sensation in UL[a]		8.3 ± 3.0	7.9 ± 3.5
Superficial sensation in LL[a]		6.6 ± 3.1	7.7 ± 3.3
Vibration sensation in UL[a]		−0.2 ± 0.4	−0.5 ± 1.0
Vibration sensation in LL[a]		−1.9 ± 1.6	−1.4 ± 1.4
Position sensation in UL[a]		−0.4 ± 1.2	−0.3 ± 0.9
Position sensation in LL[a]		−1.4 ± 1.8	−0.6 ± 1.3
Proportion of remission phase		5/12 (41.7%)*	41/60 (68.3%)
IFN beta therapy at time of SEP study		0/12 (0%)	10/60 (16.7%)
Corticosteroid at time of SEP study		11/12 (91.7%)	39/60 (65.0%)
Plasma exchange at time of SEP study		1/12 (8.3%)	2/60 (3.3%)
SEP (CSCT) UL	Unevoked	0/12 (0%)	10/60 (16.7%)
	Delayed	2/12 (16.7%)	8/60 (13.3%)
	Normal	10/12 (83.3%)	42/60 (70.0%)
SEP (CSCT) LL	Unevoked	1/12 (8.3%)	11/60 (18.3%)
	Delayed	2/12 (16.7%)	16/60 (26.7%)
	Normal	9/12 (75.0%)	33/60 (55.0%)

AQP4 = aquaporin-4; CSCT = central sensory conduction time; LL = lower limb; UL = upper limb. *$p<0.05$ in comparison between patients with and without anti-AQP4 antibody.
[a] Mean ± SD.

Table 4
Motor function and MEP findings in MS patients with and without anti-AQP4 antibody.

		Anti-AQP4 antibody - positive patients ($n=13$)	Anti-AQP4 antibody - negative patients ($n=71$)
Age at time of MEP study (years)[a]		49.5 ± 13.7*	38.9 ± 12.3
Time elapsed from disease onset to MEP study (years)[a]		5.3 ± 6.6	7.3 ± 8.4
Past and present history of muscle weakness		12/13 (92.3%)	63/71 (88.7%)
Muscle weakness in UL[a]		−0.8 ± 1.4	−0.7 ± 1.1
Muscle weakness in LL[a]		−1.5 ± 1.2	−1.5 ± 1.3
Proportion of remission phase		6/13 (46.2%)	47/71 (66.2%)
IFN beta therapy at time of MEP study		2/13 (15.4%)	16/71 (22.5%)
Steroid therapy at time of MEP study		11/13 (84.6%)	46/71 (64.8%)
Plasma exchange at time of MEP study		1/13 (7.7%)	2/71 (2.8%)
MEPs (CMCT) UL	Unevoked	5/13 (38.5%)	28/71 (39.4%)
	Delayed	1/13 (7.7%)	16/71 (22.5%)
	Normal	7/13 (53.8%)	27/71 (38.0%)
MEPs (CMCT) LL	Unevoked	4/13 (30.8%)	15/71 (21.1%)
	Delayed	3/13 (23.1%)	25/71 (35.2%)
	Normal	6/13 (46.2%)	31/71 (43.7%)

AQP4 = aquaporin-4; CMCT = central motor conduction time; LL = lower limb; UL = upper limb. *$p<0.05$ in comparison between patients with and without anti-AQP4 antibody.
[a] Mean ± SD.

3.4. MEP findings

The motor functions and MEP findings of the patients are summarized in Table 4. The degree of motor dysfunction was similar between patients with and without anti-AQP4 antibody who were subjected to MEP studies. Frequencies of immunotherapies, such as IFN beta, corticosteroids, and plasma exchange, at the time of study, were not significantly different between anti-AQP4 antibody-positive patients and anti-AQP4 antibody-negative patients. Upper limb MEPs were not evoked in five of the 13 (38.5%) patients with anti-AQP4 antibody and

Table 5
Frequency of MRI lesions in each subgroup classified according to the anti-AQP4 antibody status and evoked potential responses.

		Total	Anti-AQP4 Antibody	
			+	−
VEP (P100)[a]	Unevoked	9/41 (22.2)	4/13 (30.8)	5/28 (17.9)
	Delayed	3/51 (5.9)	1/4 (25.0)	2/47 (4.3)
	Normal	5/104 (4.8)	2/17 (11.8)	3/87 (3.4)
	Subtotal	17/196 (8.7)	7/34 (20.6)	10/162 (6.2)
SEP (CSCT)	Unevoked	14/15 (93.3)	2/2 (100.0)	12/13 (92.3)
	Delayed	16/22 (72.7)	3/3 (100.0)	13/19 (68.4)
	Normal	27/44 (61.4)	4/9 (44.4)	23/35 (65.7)
	Subtotal	57/81 (70.4)	9/14 (64.3)	48/67 (71.6)
MEPs (CMCT)	Unevoked	17/20 (85.0)	3/4 (75.0)	14/16 (87.5)
	Delayed	24/27 (88.9)	3/3 (100.0)	21/24 (87.5)
	Normal	19/39 (48.7)	3/6 (50.0)	16/33 (48.5)
	Subtotal	60/86 (69.8)	9/13 (69.2)	51/73 (69.9)

[a] Number of eyes.

Table 6
Multiple logistic analyses for possible factors contributing to severe visual impairment (finger counting or worse).

Possible factors	Severe visual impairment		OR	95% CI	p value
	+	−			
	(n=20)	(n=81)			
Male	4/20 (20.0%)	22/81 (27.2%)	3.516	(0.557–24.753)	0.182
Age of onset	31.6±13.9[a]	33.6±12.9[a]	0.964	(0.905–1.019)	0.213
Duration from onset to time of study	8.1±6.8[a]	6.7±8.4[a]	0.995	(0.892–1.096)	0.923
Anti-AQP4 antibody (+)	9/20(45.0%)	8 /81 (9.9%)	8.406	(1.547–60.125)	0.02*
Optic nerve MRI lesions	4/20 (20.0%)	7/79 (8.9%)	0.633	(0.074–4.525)	0.659
Unevoked VEP	18/20 (90.0%)	17/81 (20.1%)	35.432	(7.440–284.230)	<0.001*
Corticosteroid treatment at time of study	16/20 (80.0%)	52/81 (64.2%)	2.466	(0.427–18.231)	0.33
Plasma exchange at time of study	1/20 (5.0%)	2/81 (2.5%)	0.837	(0.024–28.101)	0.913
IFN beta therapy at time of study	7/20 (35.0%)	16/81 (19.8%)	0.914	(0.192–3.986)	0.906

*$p<0.05$.
[a] = Mean ± SD; AQP4 = aquaporin-4; CI = confidence interval; OR = odds ratio.

28 of the 71 (39.4%) patients without anti-AQP4 antibody, while one of the 13 (7.7%) patients with anti-AQP4 antibody and 16 of the 71 (22.5%) patients without the antibody showed delays in CMCT. Four of the 13 (30.8%) patients with anti-AQP4 antibody and 15 of the 71 (21.1%) patients without anti-AQP4 antibody showed a lack of evoked lower limb MEPs, while three of the 13 (23.1%) patients with AQP4 antibody and 25 of the 71 (35.2%) patients without the antibody had delayed CMCTs. There was no significant difference in the frequencies of abnormal findings between patients with and without anti-AQP4 antibody.

3.5. MRI findings

The frequencies of MRI lesions in each subgroup according to EP response and anti-AQP4 antibody status are shown in Table 5. Among patients who underwent VEP study, those who showed unevoked VEP responses had a significantly higher frequency of optic nerve lesions on MRI than those who had normal VEP responses (corrected $p=0.0105$). In patients without anti-AQP4 antibody, the frequency of optic nerve lesions on MRI tended to be higher in those with unevoked VEP responses than in those with normal VEP responses (corrected $p=0.0606$). As mentioned above, as a whole, the frequency of optic nerve lesions on MRI was significantly higher in patients with anti-AQP4 antibody than in those without the antibody ($p=0.0137$). The differences in frequencies of optic nerve lesions on MRI among subgroups classified according to VEP responses did not reach statistical significance owing to small sample size. In patients who undertook SEP study, the frequency of spinal cord lesions on MRI tended to be higher in patients with unevoked SEP responses than in those with normal SEP responses (corrected $p=0.0717$). However, no other comparisons between patients with and without anti-AQP4 antibody, or between patients with distinct SEP responses, revealed any significant difference. Among patients who were subjected to MEP study, those who demonstrated unevoked MEP responses and those who had delayed MEP responses had a significantly higher frequency of spinal cord lesions on MRI than those who had normal MEP responses (corrected $p=0.0312$ and 0.0039, respectively). In patients without anti-AQP4 antibody, those with unevoked MEP responses and those with delayed MEP responses showed a significantly higher frequency of spinal cord lesions on MRI than those with normal MEP responses (corrected $p=0.0360$ and 0.0129, respectively). There was no significant difference in the frequency of spinal cord lesions between patients with and without anti-AQP4 antibody.

3.6. Multiple logistic analyses

Among the clinical and laboratory parameters examined, only anti-AQP4 antibody positivity (OR = 8.406, $p=0.02$) and unevoked VEP response (OR = 35.432, $p<0.001$) were significantly related to the occurrence of severe visual impairment (Table 6). Disease duration from onset to time of study (OR = 1.090, $p=0.033$) and unevoked MEP response (OR = 11.013, $p=0.002$) were significantly associated with severe motor weakness in the lower limbs (Table 7). Only unevoked SEP response in the lower limbs was significantly correlated with development of severe sensory impairment in lower limbs (OR = 15.193, $p=0.004$) (other data not shown).

4. Discussion

In the present study, we disclosed that significantly more MS patients with the anti-AQP4 antibody showed a lack of VEP responses than did MS patients without the antibody, whereas delayed latency was more frequently observed in the latter group than in the former. These electrophysiological findings suggest that the nature of the lesions in the optic nerves is necrotic rather than demyelinating in anti-AQP4 antibody-positive patients compared with anti-AQP4 antibody-negative MS patients, which is in good accord with the severe visual impairment in anti-AQP4 antibody-positive patients in the present and previous

Table 7
Multiple logistic analyses for possible factors contributing to severe motor weakness in the lower limbs (moderate or worse).

Possible factors	Severe muscle weakness		OR	95% CI	p value
	+	−			
	(n=36)	(n=46)			
Male	9/36 (25.0%)	18/46 (39.1%)	0.657	(0.177–2.332)	0.518
Age of onset	34.1±14.9[a]	32.2±12.1[a]	1.044	(0.998–1.096)	0.069
Duration from onset to time of study	9.8±9.6[a]	4.9±6.1[a]	1.090	(1.013–1.190)	0.033*
Anti-AQP4 antibody (+)	5/36(13.9%)	7 /46 (15.2%)	0.424	(0.079–2.034)	0.293
Spinal cord MRI lesions	29/36 (80.6%)	29/45 (64.4%)	0.963	(0.285–3.284)	0.951
Unevoked MEP	15/36 (41.7%)	3/46 (6.5%)	11.013	(2.642–63.030)	0.002*
Corticosteroid treatment at time of study	27/36 (75.0%)	29/46 (63.0%)	1.593	(0.447–6.102)	0.478
Plasma exchange at time of study	2/36 (5.6%)	1/46 (2.2%)	1.946	(0.115–57.105)	0.651
IFN beta therapy at study	11/36 (30.1%)	7/46 (15.2%)	3.187	(0.810–13.718)	0.103

*$p<0.05$.
[a] = Mean ± SD; AQP4 = aquaporin-4; CI = confidence interval; OR = odds ratio.

studies [11]. Significant differences in age at onset were observed between anti-AQP4 antibody-positive and -negative patients. However, age at the time of VEP study and elapsed time from disease onset to the study were not different between the two groups. Moreover, multiple logistic analyses revealed that neither age at disease onset nor disease duration was significantly associated with severe visual impairment. Therefore, we do not think that the difference in age at onset significantly contributed to the worsening of VEPs in anti-AQP4 antibody-positive patients. We did not find any difference in the frequencies of abnormal findings in either SEPs or MEPs in our patients according to anti-AQP4 antibody status. This may be explained by the relatively high frequency of severe spinal cord involvement, even in anti-AQP4 antibody-negative MS patients, in Asians [1,12].

Concerning the relationship between EP abnormalities and MRI lesions, in all modalities of EPs, those who showed unevoked EP responses had higher frequencies of MRI lesions in either the optic nerve or spinal cord than those who had normal EP responses, suggesting a good concordance between electrophysiological and neuroimaging abnormalities. Regarding the relationship between anti-AQP4 antibody positivity and MRI lesions, the frequency of the optic nerve lesions on MRI was significantly higher in anti-AQP4 antibody-positive patients than in anti-AQP4 antibody-negative patients. Although the rate of detection of optic nerve lesions was not high by ordinary MRI, the higher frequency of optic nerve MRI lesions in anti-AQP4 antibody-positive patients may well reflect the severe involvement of the optic nerve in this condition. The frequency of all spinal cord lesions, including long and short lesions on MRI, was not different between patients with and without anti-AQP4 antibody; however, the frequency of LESCLs was also significantly higher in patients with anti-AQP4 antibody than in those without the antibody, probably reflecting severe inflammation and associated profuse edema in the spinal cord.

According to the multiple logistic analyses, unevoked VEP, MEP, and SEP responses were significantly correlated with severe visual, motor and sensory impairment, respectively. This indicates that unevoked EP responses reflect severe tissue destruction. Interestingly, among visual, motor and sensory impairments, anti-AQP4 antibody was found to be significantly related to only severe visual impairment by multiple logistic analyses. This suggests that some mechanism is operative to cause grave tissue damage in the optic nerve in patients carrying anti-AQP4 antibody.

We previously reported that the extensive white matter lesions occasionally seen in anti-AQP4 antibody-positive patients show a vasogenic edema pattern on diffusion-weighted MRI, with high signals on apparent diffusion coefficient maps and low signals on diffusion-weighted images [12]. We recently reported marked upregulation of proinflammatory cytokines, such as IL-17, IFN-gamma, TNF-alpha, and IL-8, in the cerebrospinal fluid of patients with the anti-AQP4 antibody [22]. Therefore, in patients harboring the anti-AQP4 antibody, vasogenic edema associated with severe inflammation is likely to occur in the CNS lesions.

AQP4 knock-out mice show amelioration of cytotoxic edema [27] but worsening of vasogenic edema [28] suggesting an important role of AQP4 molecules in the resolution of vasogenic edema. As anti-AQP4 antibody induces down-modulation of AQP4 molecules in AQP4-transfected cultured cells [29], loss of AQP4 on astrocyte foot processes in vivo may retard the resolution of vasogenic edema. If anti-AQP4 antibodies are promptly removed by plasma exchange or extracellular fluid volume is reduced by corticosteroids, such edematous lesions may fade away leaving no major deficits in either myelopathy or encephalopathy, probably through recycling of AQP4 molecules and repair of astrocyte foot processes [29]. By contrast, in the case of the optic nerve, the compensatory space for distension is extremely small, being smallest at the orbital end [30], and the blood is supplied only from the anastomosed small vessels between the dural and pial vessel systems [31]. Therefore, once the optic nerve inflammation extends to the anterior portion of the canal, vasogenic edema accompanied by inflammation easily causes optic nerve ischemia, resulting in severe residual visual impairment [32]. The occurrence of such a secondary ischemic optic neuropathy owing to tissue edema is well known in a variety of conditions, such as minor head trauma, craniofacial surgery, hemorrhage, tumors, and intracranial hypertension [30–34]. Therefore, it is easily conceivable that prolonged vasogenic edema accompanied by the optic neuritis may produce obstruction of small vessels at the optic canal, and cause ischemic necrosis of the optic nerve in anti-AQP4 antibody-positive patients. This assumption may well explain the observation that NMO-IgG is significantly associated only with severe visual impairment [11].

The present study disclosed a high frequency of patients with anti-AQP4 antibody lacking VEP responses, suggesting critical roles for the antibody in severe optic nerve impairment. A delay in the initiation of immunological treatment for this condition may lead to a loss of visual function. These observations thus warrant prompt immunological treatment, such as plasma exchange and intravenous immunoglobulin administration, in patients with anti-AQP4 antibody who show optic nerve involvement.

Acknowledgments

This work was supported in part by grants from the Research Committees of Neuroimmunological Diseases, the Ministry of Health, Labour and Welfare, Japan, and from the Ministry of Education, Culture, Sports, Science and Technology, Japan.

References

[1] Kira J. Multiple sclerosis in the Japanese population. Lancet Neurol 2003;2: 117–27.
[2] Kira J, Kanai T, Nishimura Y, Yamasaki K, Matsushita S, Kawano Y, et al. Western versus Asian types of multiple sclerosis: immunogenetically and clinically distinct disorders. Ann Neurol 1996;40: 569–74.
[3] Wingerchuk DM, Hogancamp WF, O'Brien PC, Weinshenker BG. The clinical course of neuromyelitis optica (Devic's syndrome). Neurology 1999;53: 1107–14.
[4] Cree BA, Goodin DS, Hauser SL. Neuromyelitis optica. Semin Neurol 2002;22: 105–22.
[5] Lucchinetti CF, Mandler RN, McGavern D, Bruck W, Gleich G, Ransohoff RM, et al. A role for humoral mechanisms in the pathogenesis of Devic's neuromyelitis optica. Brain 2002;125: 1450–61.
[6] Yamasaki K, Horiuchi I, Minohara M, Kawano Y, Ohyagi Y, Yamada T, et al. HLA-DPB1*0501-associated opticospinal multiple sclerosis: clinical, neuroimaging and immunogenetic studies. Brain 1999;122: 1689–96.
[7] Ishizu T, Osoegawa M, Mei FJ, Kikuchi H, Tanaka M, Takakura Y, et al. Intrathecal activation of the IL-17/IL-8 axis in opticospinal multiple sclerosis. Brain 2005;128: 988–1002.
[8] Lennon VA, Kryzer TJ, Pittock SJ, Verkman AS, Hinson SR. IgG marker of optic-spinal multiple sclerosis binds to the aquaporin-4 water channel. J Exp Med 2005;202: 473–7.
[9] Lennon VA, Wingerchuk DM, Kryzer TJ, Pittock SJ, Lucchinetti CF, Fujihara K, et al. A serum autoantibody marker of neuromyelitis optica: distinction from multiple sclerosis. Lancet 2004;364: 2106–12.
[10] Wingerchuk DM, Lennon VA, Pittock SJ, Lucchinetti CF, Weinshenker BG. Revised diagnostic criteria for neuromyelitis optica. Neurology 2006;66: 1485–9.
[11] Nakashima I, Fujihara K, Miyazawa I, Misu T, Narikawa K, Nakamura M, et al. Clinical and MRI features of Japanese patients with multiple sclerosis positive for NMO-IgG. J Neurol Neurosurg Psychiatry 2006;77: 1073–5.
[12] Matsuoka T, Matsushita T, Kawano Y, Osoegawa M, Ochi H, Ishizu T, et al. Heterogeneity of aquaporin-4 autoimmunity and spinal cord lesions in multiple sclerosis in Japanese. Brain 2007;130: 1206–23.
[13] Weinshenker BG, Wingerchuk DM, Nakashima I, Fujihara K, Lennon VA. OSMS is NMO, but not MS: proven clinically and pathologically. Lancet Neurol 2006;5: 110–1.
[14] Roemer SF, Parisi JE, Lennon VA, Benarroch EE, Lassmann H, Bruck W, et al. Pattern specific loss of aquaporin-4 immunoreactivity distinguishes neuromyelitis optica. Brain 2007;130: 1194–205.
[15] Misu T, Fujihara K, Kakita A, Konno H, Nakamura M, Watanabe S, et al. Loss of aquaporin-4 in lesions of neuromyelitis optica: distinction from multiple sclerosis. Brain 2007;130: 1224–34.
[16] Jacob A, Matiello M, Wingerchuk DM, Lucchinetti CF, Pittock SJ, Weinshenker BG. Neuromyelitis optica: changing concepts. J Neuroimmunol 2007;187: 126–38.
[17] Chong HT, Ramli N, Lee KH, Kim BJ, Ursekar M, Dayananda K, et al. Magnetic resonance imaging of Asians with multiple sclerosis was similar to that of the West. Can J Neurol Sci 2006;33: 95–100.
[18] Su JJ, Osoegawa M, Matsuoka T, Monihara M, Tanaka M, Ishizu T, et al. Upregulation of vascular growth factors in multiple sclerosis: correlation with MRI findings. J Neurol Sci 2006;243: 21–30.

[19] Minohara M, Matsuoka T, Li W, Osoegawa M, Ishizu T, Ohyagi Y, et al. Upregulation of myeloperoxidase in patients with opticospinal multiple sclerosis: positive correlation with disease severity. J Neuroimmunol 2006;178: 156–60.
[20] Matsuoka T, Matsushita T, Osoegawa M, Ochi H, Kawano Y, Mihara F, et al. Heterogeneity and continuum of multiple sclerosis in Japanese according to magnetic resonance imaging findings. J Neurol Sci 2008;266: 115–25.
[21] Bot JC, Barkhof F, Polman CH, Lycklama à Nijeholt GJ, de Groot V, Bergers E, et al. Spinal cord abnormalities in recently diagnosed MS patients: added value of spinal MRI examination. Neurology 2004;62: 226–33.
[22] Tanaka K, Tani T, Tanaka M, Saida T, Idezuka J, Yamazaki M, et al. Anti-aquaporin 4 antibody in selected Japanese multiple sclerosis patients with long spinal cord lesions. Mult Scler 2007;13: 850–5.
[23] Poser CM, Paty DW, Scheinberg L, McDonald WI, Davis FA, Ebers GC, et al. New diagnostic criteria for multiple sclerosis: guidelines for research protocols. Ann Neurol 1983;13: 227–31.
[24] Kurtzke JF. Rating neurologic impairment in multiple sclerosis: an expanded disability status scale (EDSS). Neurology 1983;33: 1444–52.
[25] Tobimatsu S, Fukui R, Kato M, Kobayashi T, Kuroiwa Y. Multimodality evoked potentials in patients and carriers with adrenoleukodystrophy and adrenomyeloneuropathy. Electroencephalogr Clin Neurophysiol 1985;62: 18–144.
[26] Pineda AA, Ogata K, Osoegawa M, Murai H, Shigeto H, Yoshiura T, et al. A distinct subgroup of chronic inflammatory demyelinating polyneuropathy with CNS demyelination and a favorable response to immunotherapy. J Neurol Sci 2007;255: 1–6.
[27] Manley GT, Fujimura M, Ma T, Noshita N, Filiz F, Bollen AW, et al. Aquaporin-4 deletion in mice reduces brain edema after acute water intoxication and ischemic stroke. Nat Med 2000;6: 159–63.
[28] Papadopoulos MC, Manley GT, Krishna S, Verkman AS. Aquaporin-4 facilitates reabsorption of excess fluid in vasogenic brain edema. FASEB J 2004;18: 1291–3.
[29] Hinson SR, Pittock SJ, Lucchinetti CF, Roemer SF, Fryer JP, Kryzer TJ, et al. Pathogenic potential of IgG binding to water channel extracellular domain in neuromyelitis optica. Neurology 2007;69: 2221–31.
[30] Tao H, Ma Z, Dai P, Jiang L. Computer-aided three-dimensional reconstruction and measurement of the optic canal and intracanalicular structures. Laryngoscope 1999;109: 1499–502.
[31] Thale A, Jungmann K, Paulsen F. Morphologic studies of the optic canal. Orbit 2002;21: 131–7.
[32] Cerovski B, Sikic J, Juri J, Petrovic J. The role of visual evoked potentials in the diagnosis of optic nerve injury as a result of mild head trauma. Coll Antropol 2001;25: 47–55 [Suppl].
[33] Girotto JA, Gamble WB, Robertson B, Redett R, Muehlberger T, Mayer M, et al. Blindness after reduction of facial fractures. Plast Reconstr Surg 1998;102: 1821–34.
[34] Acheson JF. Optic nerve disorders: role of canal and nerve sheath decompression surgery. Eye 2004;18: 1169–74.

Laboratory Investigation

Stereotactic and Functional Neurosurgery

Stereotact Funct Neurosurg 2009;87:211–218
DOI: 10.1159/000225974

Published online: June 26, 2009

Spectral Analysis of Field Potential Recordings by Deep Brain Stimulation Electrode for Localization of Subthalamic Nucleus in Patients with Parkinson's Disease

Yasushi Miyagi[a, b] Tsuyoshi Okamoto[a] Takato Morioka[b] Shozo Tobimatsu[c] Yoshitaka Nakanishi[a] Kazuyuki Aihara[d] Kimiaki Hashiguchi[b] Nobuya Murakami[e] Fumiaki Yoshida[b] Kazuhiro Samura[b] Shinji Nagata[b] Tomio Sasaki[b]

[a]Digital Medicine Initiative and Departments of [b]Neurosurgery and [c]Clinical Neurophysiology, Graduate School of Medical Sciences, Kyushu University, [d]Aihara Complexity Modeling Project, ERATO, JST, and [e]Department of Neurosurgery, Kaizuka Hospital, Fukuoka, Japan

Key Words

Oscillatory synchrony · Subthalamic nucleus · Local field potential · Spectral density analysis · β-Activity · Deep brain stimulation · Parkinson's disease

Abstract

Aims: Spectral analysis of local field potential (LFP) recorded by deep brain stimulation (DBS) electrode around the subthalamic nucleus (STN) in patients with Parkinson's disease was performed. ***Methods:*** The borders of the STN were determined by microelectrode recording. The most eligible trajectory for the sensorimotor area of the STN was used for LFP recording while advancing the DBS electrode. ***Results:*** The low-frequency LFP power (θ- to β-band) increased from a few millimeters above the dorsal border of the STN defined by microelectrode recording; however, the low-frequency power kept the same level beyond the ventral border of the STN. Only high β-power showed close correlation to the dorsal and ventral borders of the STN. ***Conclusions:*** A spectral power analysis of LFP recording by DBS electrode helps with the final confirmation of the dorsal and ventral borders of the STN of Parkinson's disease in DBS implantation surgery.

Introduction

In Parkinson's disease (PD), it is postulated that dopamine depletion in the striatum leads to an oscillatory synchrony in low-frequency (β-band) neuronal discharges of the basal ganglia [1]. Such oscillatory synchrony is considered to induce the antikinetic effect on the interaction between the motor cortex and basal ganglia in the 'off' state of PD, but when the patient's motor function is turned to the 'on' state by levodopa treatment, the β-band oscillation disappears or changes into γ-band oscillation [2].

KARGER

Fax +41 61 306 12 34
E-Mail karger@karger.ch
www.karger.com

1011–6125/09/0874–0211$26.00/0

Accessible online at:
www.karger.com/sfn

Yasushi Miyagi, MD, PhD
Division of Digital Patient, Digital Medicine Initiative, Kyushu University
3-1-1 Maidashi, Higashi-ku, Fukuoka, 812-8582 (Japan)
Tel. +81 92 642 6693, Fax +81 92 642 6693
E-Mail yamiyagi@digital.med.kyushu-u.ac.jp

In some studies on local field potential (LFP) in the basal ganglia, a low-impedance microelectrode was used during stereotactic neurosurgery [3–5]. However, the LFPs can be recorded using a deep brain stimulation (DBS) electrode during surgery [6–8] or during the trial period after implantation with an externalized cable [7, 9]. Chen et al. [6] reported that the subthalamic nucleus (STN) can be physiologically localized by DBS electrode alone, without performing microelectrode recording (MER). In their study a DBS electrode was inserted by a 2-mm step. When the contact got into the STN, a spectral change was observed. However, the details of the border of the STN were not identifiable with the 2-mm step insertion. Since the depth of the dorsal and ventral borders defines the physiological width of the STN, which is considered a major determinant of the eligible trajectory for the implantation of a DBS electrode [10, 11], the detailed characteristics of LFP around the dorsal and ventral borders provide crucial information if MER is not performed. The purpose of this study is to characterize the LFP changes around the STN borders, and to identify the dorsal and ventral STN border by the change in LFP from the DBS electrode.

Materials and Methods

Patients

Nine STNs from 7 patients with idiopathic PD (2 males and 5 females, with a mean age of 65 ± 5.3 years ranging from 50 to 71) were included for the LFP recording during DBS surgery. All patients had disabling motor fluctuations and/or levodopa-induced dyskinesia refractory to the adjustment of antiparkinsonian medication. The mean disease duration was 14 ± 8.5 years, and the mean Hoehn-Yahr stage was 3.9 ± 1.1 in the 'off' state and 2.7 ± 0.8 in the 'on' state. The patients were treated with levodopa and dopamine agonists; the daily dose of levodopa was 586 ± 306 mg/day (total levodopa equivalent dose = 884 ± 458 mg/day). In 5 patients, only unilateral STN was explored for LFP recording because of limited operation time.

Surgical Procedure

All patients gave their informed consent for DBS implantation surgery and related data acquisition. Surgeries were performed in the 'off' state after an 18-hour discontinuation of antiparkinsonian medication. After a stereotactic head frame (Leksell model G, Elekta) had been affixed to the patient's head under local anesthesia, the patient underwent preoperative magnetic resonance (MR) imaging and helical computerized tomography (CT). The axial images were transferred to the workstation computer in the operating room in a DICOM format. The data were imported into the computer software SurgiPlan™ (Elekta, Sweden). After both 3-dimensional images reconstructed from MR and CT had been exactly matched, as confirmed by the image fusion tool, the coordinates of the anterior and posterior commissures (AC and PC) were directly calculated by the software. The theoretical target was placed 11–12 mm lateral to the AC-PC line, 3 mm posterior and 5 mm ventral to the midcommissural point. The laterality of the theoretical target from the AC-PC line was also individually modified, as 3 mm lateral to the lateral border of the red nucleus visualized on a T_2-weighted coronal image in each case. The coordinates were also calculated separately by manual drawing on the X-ray film, and a consensus was obtained with the results from the 'functional target' tool of SurgiPlan. The entry point (site of burr hole) was placed around the coronal suture and 3–4 cm lateral to the midline; the final trajectory was planned to avoid the cortical sulci and lateral ventricle. The patient's head with head frame was secured to the operating table, and the patient was postured in a supine position to prevent a brain shift during the burr hole surgery [12].

Multitrack Microrecording

A semicircular skin incision and burr hole were made at the entry point. Immediately after the dura mater had been opened, the burr hole was covered with fibrin glue to prevent the outflow of cerebrospinal fluid during surgery. Four cannulae for multitrack MER (Array electrode insertion tube®, Medtronic Inc., Minneapolis, Minn., USA) were inserted into the cortex. The STN was physiologically localized by 4 simultaneously inserted tracks of microelectrode (microTargeting Electrode®, Medtronic) [13]. MER was started 15 mm above the theoretical target and conducted by a manual microdrive device. Extracellular potentials were sampled at a rate of 24 kHz by a surgical monitoring system (Leadpoint®, Medtronic) and the data were collected every 10 s at each depth. The discharge pattern of the neurons of the subthalamus and substantia nigra pars reticulata (SNr) could be identified as follows: characteristic neuronal discharges of the STN were identified by the robust increase in background activity with multiple units with a relatively large amplitude and nontonic irregular discharge pattern with a firing rate of around 30–60 Hz. As the electrode went beyond the STN, the background activity substantially decreased and the SNr cells with high-frequency and tonic discharges appeared. The boundary between STN and SNr was not always clear; therefore, the ventral border of the STN was defined by offline analysis. The sensorimotor area of the STN was distinguished by the modification of neuronal discharges in response to active and passive joint movement of contralateral limbs. The track recording the sensorimotor response of the STN and a width of STN larger than 4 mm was regarded as the eligible trajectory for DBS electrode implantation [10, 11, 14].

LFP Recording by DBS Electrode

After the dorsal and ventral borders of the STN had been identified by MER, the DBS electrode (model 3389, Medtronic) with 4 platinum-iridium cylindrical surfaces (1.27 mm diameter with 1.5 mm length) and 0.5-mm intervals was introduced to the microdrive device. The DBS electrode was mounted to keep a spatial relationship so that the center between the 2 lowermost bipolar contacts coincided with the depth of the microelectrode tip. LFPs were recorded by use of the LeadPoint system, too. The sensitivity was adjusted to 0.1 mV per dot in the display and the sampling rate was 24 kHz. Using the lowermost 2 contacts (contact 0 and contact 1), the LFP was recorded from 15 mm above the theoretical target down to 5 mm beyond the theoretical target in a 1-mm

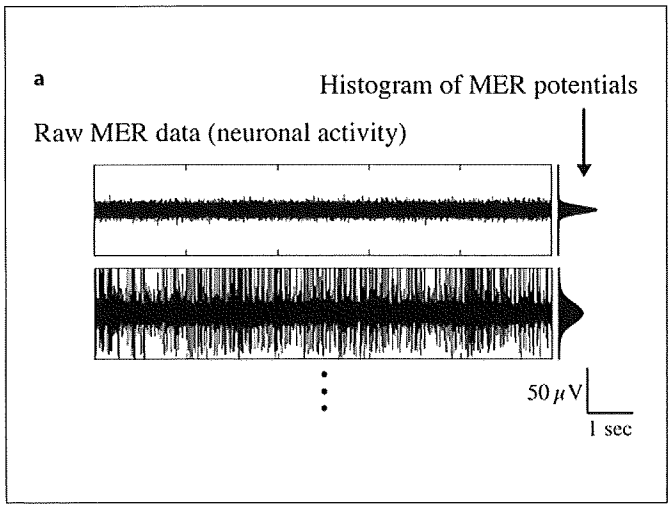

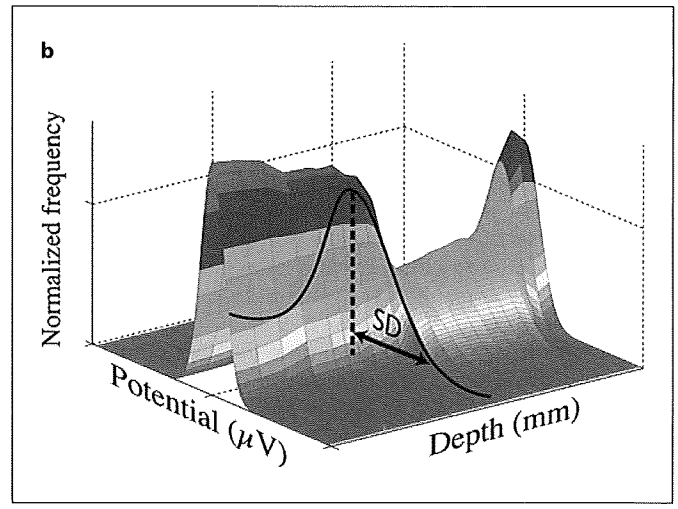

Color version available online

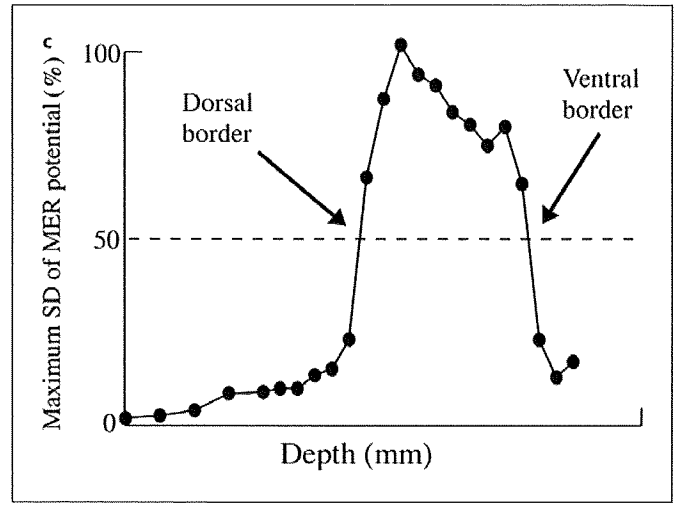

Fig. 1. Method of offline analysis of MER in determining the electrophysiological border of the STN. **a** The SD of 240,000 data points (24 kHz for 10 s) of MER potential was regarded as a background activity of each depth. **b** The relationship between the histogram of MER potential and the depth of each microelectrode. **c** The SD of MER potentials at each depth was expressed as a percentage of maximum SD in each patient and the depths where percent SD increased up to 50% and subsequently decreased down to 50% were defined as dorsal and ventral borders of the STN, respectively.

step with filtration of 1–50 Hz. The patients were kept at rest without any voluntary movement during LFP recording because the degree of synchronization of STN neurons in the β-band is dependent on patients' movement [9, 15]. The DBS electrode was not advanced further than 5 mm from theoretical target.

Macrostimulation and Implantation

The DBS electrode was withdrawn to the depth where the lowermost 2 contacts were located within the STN as determined by MER, and the electrode location was confirmed by intraoperative roentgenogram. The parameters used for macrostimulation by DBS electrode were as follows: bipolar stimulation with contact 1 (dorsal half of the STN) as cathode and contact 3 as anode, pulse width 60 μs, frequency 130 Hz. The muscle rigidity was significantly decreased by insertion of the DBS electrode even in the absence of electrical stimulation (microlesioning effect). In all cases, the amplitude could be gradually increased up to 5.0 V without the generation of adverse effects, such as dysarthria, conjugate deviation or dystonic muscle contraction. After getting the optimal therapeutic effect by the refinement of the electrode position, the electrode was fixed with the Medtronic burr hole cap. The final position of the electrode tip was consistently ascertained by intraoperative roentgenogram. The same procedure was then repeated for the other side. Finally, the patients underwent the implantation of an extension cable and an internal pulse generator under general anesthesia on the same day.

Frequency Analysis

Since the high background neuronal activity reflects both high-frequency spikes and high neuronal density, the changes in the histogram of MER potentials are considered to correlate with both the neuronal density of the STN and the spiking activity of neurons. Therefore, the standard deviation (SD) of 240,000 data points (24 kHz for 10 s) of MER potential was regarded as a background activity at each depth and used as an electrophysiological marker of STN (fig. 1a, b). The background activity began to increase a few millimeters above the estimated dorsal border before it turned into a steep increase in each trajectory. In order to avoid the vagueness of the STN border in this study, the SD of MER potentials at each depth was expressed as a percentage of the maxi-

mum SD in each patient, and the depths where the SD increased up to 50% of maximum and subsequently decreased down to 50% of maximum were defined as the dorsal and ventral borders of STN, respectively (fig. 1c).

The power spectral density (PSD) was calculated by Fourier transform with Welch's modification [16] over the 10-second sequence of LFP which is segmented into 1-second sections overlaid with a Hamming window, each with a 50% overlap. In the spectral density analysis of LFP around the dorsal border of the STN, 9 data sets of MER and LFP records were aligned while assuming the depth of the dorsal border as 0 mm. In case of LFP analysis around the ventral border of the STN, 9 data sets of MER and LFP records were realigned while assuming the depth of the ventral border as 0 mm. The maximum power was obtained in each band of θ (4–7 Hz), α (8–13 Hz) and β (14–35 Hz). In particular, the β-band was further divided into low β (14–20 Hz) and high β (21–35 Hz). The relationships between the DBS electrode depth to the dorsal and ventral borders of the STN determined by MER and the LFP power of each band recorded by DBS electrode were analyzed.

Statistical Analysis and Ethical Aspects

The LFP response recorded by DBS electrode is related to the level of activity of large groups of neurons. The PSD change of LFP with the depth does not always show the same trend as the background activity recorded by MER electrode. In order to test the significance of PSD increase and decrease of LFP with the location of the electrode, the correlation analysis between the normalized PSD and the depth of the electrode located between –2 and 2 mm around the ventral border or dorsal border of the STN, respectively, was performed. In this analysis, both the correlation coefficient R and the p value for testing the hypothesis of no correlation were calculated in each band of θ, α and β. If the p value is less than 0.05, then the correlation coefficient R is significant. This study was approved by the Research Ethics Committee, Kyushu University (No. 20–16).

Results

The width of the STN determined by MER was 5.2 ± 0.6 mm along the eligible track for DBS electrode implantation. Figure 2 shows the representative records of a 65-year-old male patient indicating the dependency of PSD on the depth of the DBS electrode from dorsal to ventral of the STN through the trajectory, including the sensorimotor area detected by multitrack MER. The power of the low-frequency band clearly increased around the dorsal border of the STN at –4 mm to the tentative target (0 mm depth) in figure 2 and low-frequency synchrony was kept at the same level beyond the ventral border of the STN; only the high β-power of LFP showed a clear decrease around the ventral border.

The summary of 10 LFP recordings is shown in figure 3, in which the depth-power relationships were aligned in reference to the dorsal (fig. 3b–e) and ventral (fig. 3g–j) borders, which are designated as 0 mm depth, respectively. Although the background activity in all MER data showed a steep increase around the dorsal border of the STN (fig. 3a), the LFP power of each low-frequency band began to increase from a few millimeters above the dorsal border. As a whole, the depth at which θ-, α- and low β-powers reached almost half of the maximum power coincided with the dorsal border (depth 0 mm); at the depth of 2 mm dorsal to the STN, however, only high β-power reached half of the maximum power ($R = 0.48$, $p < 0.001$, fig. 3e). As the DBS electrode advanced ventrally, the LFP power appeared to increase within the STN or remained the same, and when aligned by the ventral border of the STN, the LFP power of the θ- to low β-band did not show any significant change around the ventral border (depth 0 mm). Only the high β-power showed a small but significant decline just at the ventral border ($R = -0.37$, $p = 0.01$, fig. 3j).

Discussion

In this study, we performed an LFP recording from a DBS electrode to detect any change in spectral density of LFP specific to the borders of the STN along the trajectory of the DBS electrode. An approximate 50% increase from the baseline in the LFP power of low-frequency (θ- to low β-) bands correlated with the dorsal STN border. However, the LFP power of these bands did not show any significant change around the ventral border. Therefore, the increase in oscillatory activity in a low-frequency band is clear when the DBS electrode moves from Forel's field or the zona incerta into the dorsal STN, while the decrease in oscillatory activity is unclear around the ventral STN. These results suggest that low-frequency LFP power recording by DBS electrode can be used only for the detection of the dorsal border of the STN and the high β-power of LFP can help detect the ventral border of the STN.

Dopaminergic depletion in the striatum induces the β-band oscillatory synchrony of neuronal activity in the STN and globus pallidus internus, which contributes to the antikinetic effect on the basal ganglia in the 'off' state of PD [1]. The use of β-power of LFP is reasonable for the electrophysiological localization of the STN [6, 4]. An LFP recording by a DBS electrode has several technical problems to be overcome. A simultaneous recording of LFP and neuronal discharge revealed that the mean β-power (13–35 Hz) was greater in the dorsolateral than in the ventromedial STN [3], and a majority of β-oscillatory